Numerical analysis of the Monte-Carlo noise for the resolution of the deterministic and uncertain linear Boltzmann equation (comparison of non-intrusive gPC and MC-gPC)

Gaël Poëtte

Numerical analysis of the Monte-Carlo noise for the resolution of the deterministic and uncertain linear Boltzmann equation (comparison of non-intrusive gPC and MC-gPC)

Gaël Poëtte[a]

[a] *CEA DAM CESTA, F-33114 Le Barp, France*

Abstract

Monte Carlo-generalised Polynomial Chaos (MC-gPC) has already been thoroughly studied in the literature [1, 2, 3, 4, 5, 6, 7]. MC-gPC both builds a gPC based reduced model of a partial differential equation (PDE) of interest and solves it with an intrusive MC scheme in order to propagate uncertainties. This reduced model captures the behaviour of the solution of a set of PDEs subject to some uncertain parameters modeled by random variables. MC-gPC is an intrusive method, it needs modifications of a code in order to be applied. This may be considered a drawback. But, on another hand, important computational gains obtained with MC-gPC have been observed on many (linear [1, 3] or nonlinear [4, 5, 6, 7]) applications. The MC-gPC resolution of Boltzmann equation has been investigated in many different ways: the wellposedness of the gPC based reduced model has been studied in [2, 6], the convergence with respect to the truncation order P has been theoretically and numerically studied [2, 1], the coupling to nonlinear physics has been performed in [7, 6]. But *the study of the MC noise remains, to our knowledge, to be done.* This is the purpose of this paper.

Keywords: Monte Carlo, generalised Polynomial Chaos, Uncertainty Quantification, Transport

1. Introduction

Monte Carlo-generalised Polynomial Chaos (MC-gPC) has already been thoroughly studied in the literature [1, 2, 3, 4, 5, 6, 7]. MC-gPC both builds a gPC based reduced model of a partial differential equation (PDE) of interest and solves it with an MC scheme in order to propagate uncertainties. This reduced model captures the behaviour of the solution of a set of PDEs subject to some uncertain parameters modeled by random variables. MC-gPC is an intrusive method, it needs modifications of an MC code in order to be applied. This may be considered a drawback. But, on another hand, important computational gains obtained with MC-gPC have been observed on many (linear [1, 3] or nonlinear [4, 5, 6, 7]) applications. Its use allows performing studies (uncertainty propagation, sensitivity analysis etc.) which, up to now, were out of reach [1, 7, 6]. In this article, we are interested in the MC resolution of the gPC based reduced model of the uncertain

Email address: gael.poette@cea.fr (Gaël Poëtte)

linear transport equation

$$\begin{aligned}\partial_t u(x,t,v,X) + v\cdot\nabla_x u(x,t,v,X) = &- v\sigma_t(x,v,X)u(x,t,v,X)\\ &+ v\sigma_s(x,v,X)\int P_s(x,v\cdot v',X)u(x,t,v',X)\,\mathrm{d}v',\end{aligned} \tag{1}$$

together with the initial and boundary conditions

$$\begin{array}{l} u(x,t=0,v,X) = u_0(x,v,X), \quad x\in\mathcal{D}(X), \quad t\in[0,T] \quad v\in\mathcal{V}, \quad X\in\Omega \\ u(x,t,v,X) = u_b(t,v,X), \quad x\in\partial\mathcal{D}(X), \quad t\in[0,T] \quad v\cdot n_s(x,X)<0, \quad X\in\Omega, \end{array} \tag{2}$$

where n_s is the outward normal to Ω at x. In the above expression, u is a density of particles. The variables $x\in\mathcal{D}\subset\mathbb{R}^3$, $t\in[0,T]\subset\mathbb{R}^+$ and $v\in\mathcal{V}\subset\mathbb{R}^3$ are respectively the space, time and velocity[1] variables. Variable $X=(X_1,...,X_Q)^t$ is a vector of Q independent[2] random variables of probability measure $\mathrm{d}\mathcal{P}_X=\prod_{i=1}^Q \mathrm{d}\mathcal{P}_{X_i}$ modelling the uncertainties. Variables (x,t,v) are the *physical* variables in opposition to X which is refered to as the *uncertain* variable. The cross-sections $\sigma_t=\sigma_t(x,v,X)$, $\sigma_s=\sigma_s(x,v,X)$ are assumed to be given functions of (x,v,X) in this paper. They stand for the total and scattering cross-sections. The quantity P_s defines how the velocities and angles are scattered when a reaction is encountered: it (at least) satisfies $\int P_s(x,v\cdot v',X)\,\mathrm{d}v'=1, \forall x\in\mathcal{D}, v\in\mathcal{V}\in\mathbb{R}^3, X\in\Omega\subset\mathbb{R}^Q$. Of course, the above notations are for macroscopic cross-sections, in the sense that many physical reactions are summed-up in the above notations, see [13, 14, 15]. System (1) together with boundary conditions (2) define the well-posed [16] mathematical problem we want to solve and in which we want to *be able to accurately take uncertainties*[3] *into account*. In other words, we are mainly interested in the statistics of $X\to u(x,t,v,X)$ (i.e. mean, variance, histogram, sensitivity indices [17] etc.) at specified locations $x\in\mathcal{D}$, times $t\in[0,T]$ and velocities $v\in\mathcal{V}$. The uncertain transport equation is of importance in many physical domains such as neutronics [18, 19, 20, 7], photonics [21, 22, 23, 24, 25, 6], biology [26], socio-economics [5, 27, 3], epidemiology [28] etc. In neutronics [7] or photonics [6] for example, equation (1) must be solved at each iteration/time step.

Of course, different values of X correspond to different fully decoupled deterministic equations: in principle, there is no difficulty in solving such uncertain problem. The main issue comes from the fact that exact propagation of uncertainties is very expensive from the computational point of view: equation (1) is often solved thanks to an MC scheme [29, 18, 30, 19, 20, 31, 32, 33]. This resolution method is known to be efficient for high $(3(x)+1(t)+3(\mathbf{v})=7)$ dimensional problems but costly. Running several deterministic MC computations for several values of X can consequently be prohibitive.

Recently, a new solver, called MC-gPC, has been proposed in order to solve the uncertain linear Boltzmann equation (1): it is based on the construction of a $P-$truncated gPC based reduced model together with its MC resolution [1]. The idea of MC-gPC is to make the MC particles solve not only the physical fields (x,t,v) but also the uncertain one X, *on-the-fly* during the MC resolution (it then avoids tensorising the physical and the uncertain experimental designs, see [1]). To sum-up,

[1] It may be decomposed into $v=v\omega$ where $v=|v|\in\mathbb{R}^+$ and $\omega=\frac{v}{v}\in\mathbb{S}^2$.

[2] It is always possible to come back to such framework, at the cost of more or less tedious pretreatments leading to a controled approximation [8, 9, 10] and decorrelation [11, 12].

[3] geometrical, in the cross-sections, in the multiplicity, in the boundary conditions etc.

important gains have been observed in low to moderate stochastic dimensions[4] $Q \sim 1-10$ with *simple* modifications of an existing MC code and *without changing* the HPC strategy[5] of the code, for linear [1, 2], nonlinear [6] and eigenvalue (k_{eff}) [7] problems.

The MC-gPC resolution of equation (1) has been investigated in many different ways: the wellposedness of the gPC based reduced model has been studied in [2, 6], the convergence with respect to the truncation order P has been theoretically and numerically studied [2, 1], the coupling to nonlinear physics has been performed in [7, 6]. But *the study of the MC noise remains, to our knowledge, to be done.* This is the purpose of this paper. In this paper, we are interested in understanding what can be expected in terms of error estimations with respect to N_{MC}, the number of MC particles. Typically, we try to give elements of answers to the following question: what can be expected in terms of MC noise for MC-gPC when compared to a more classical (i.e. non-intrusive) application? In order to answer that question, we estimate the variances of non-intrusive gPC and MC-gPC, theoretically and numerically, and compare them. Of course, the studies could only have been carried out numerically (by performing several fine MC resolutions and comparing the results) but the performances of the different resolution schemes can be very similar hence hard to distinguish due to the noise. For this reason, in order to avoid misleading situations, we also focus on simple regimes (free flight regime, collisional regime) for which analytical calculations of the asymptotical errors are possible.

The paper is organized as follows: section 2 recalls the main principles of non-intrusive gPC and MC-gPC for solving (1) and introduce notations. In section 3, we present asymptotical results on some commonly implemented deterministic MC scheme allowing to solve (1) non-intrusively. Several other MC schemes exist, see [29, 15, 34] and the references therein, but we can not go through every of them. We focus on the semi-analog scheme[6], intensively used in neutronic codes[7] [18, 19, 20], and on the non-analog one, mainly used in photonic ones [36, 21, 22, 37, 38, 39, 40]. Even for those well-known MC schemes, the analysis made in this section is, to our knowledge, original. In section 4, the numerical analysis of the amplitude of the noise (i.e. the variance as an error estimator) of the uncertain MC schemes, non-intrusive gPC vs. MC-gPC resolutions for (1), are performed in the same conditions as in section 3 and compared. Emphasis is made on verification (as in Verification & Validation, see V&V [41]) in those two sections 3–4. Section 5 is devoted to discussions on how to use the previous material in practice together with concluding remarks on how MC-gPC could be improved. Note that we chose to add in the appendices all the material which one can find in other papers but which eases the understanding and the reproducibility of the results of this paper.

[4] MC-gPC being based on gPC which is sensitive to the curse of dimension, the $P-$truncated reduced models remains exponentially sensitive to P and Q, see [1, 2].

[5] The HPC strategy we have in mind is commonly called *domain replication*, see [31, 32, 33]. It consists in replicating the geometry on several processors and tracking several MC particles populations with different initial seeds in every replicated domains. At the end of the time steps, the contribution of every processors are averaged. This parallel strategy is particularly well suited to MC codes, taking advantage of the independence of the MC particles.

[6] Also known as *implicit capture*.

[7] Note that this MC scheme is also intensively used in photonics, see [35, 24, 25].

2. Non-intrusive gPC and MC-gPC reduced models in a nutshell

In this paper, we are interested in the construction of gPC based reduced models in order to take into account uncertainties. Let us introduce the polynomials basis $(\phi_k^X)_{k\in\mathbb{N}}$ orthonormal with respect to the scalar product defined by $\mathrm{d}\mathcal{P}_X$, i.e such that

$$\int \phi_k^X(X)\phi_l^X(X)\,\mathrm{d}\mathcal{P}_X = \delta_{k,l}, \forall (k,l)\in\mathbb{N}^2.$$

In practice, this basis is built once and for all once $\mathrm{d}\mathcal{P}_X$ known. In the above expression, the basis must be truncated up to certain orders $(p_i)_{i\in\{1,...,Q\}}$ which may depend on the directions $(X_i)_{i\in\{1,...,Q\}}$. Assume that $\forall i\in\{1,..,Q\}$, $p_i = p_{1\mathrm{D}}$, then the total number of polynomial coefficients, abusively called the polynomial order later on, is[8] $P = P(p_{1\mathrm{D}}, Q) = (p_{1\mathrm{D}}+1)^Q$. It exhibits an exponential growth with both $p_{1\mathrm{D}}$ and Q. This is commonly called *the curse of dimensionality* [43, 44]. As a consequence, the reduced models described in this paper, in practice, can only be applied to a moderate number of uncertain parameters ($Q\sim 10$). The multivariate polynomial basis is built by tensorization of one-dimensional polynomial basis in every stochastic direction $(X_i)_{i\in\{1,...,Q\}}$. In the following sections, for conciseness in the notations, we map[9] the set of polynomial indices $\mathcal{A}^{p_{1\mathrm{D}},Q} = \{(k_1,...k_Q)|\forall i\in\{1,...,Q\}, k_i\le p_{1\mathrm{D}}\}$ into $\{0,...,P\}$ to build the tensorized basis $(\phi_k^X(X) = \prod_{i=1}^Q \phi_{k_i}^{X_i}(X_i))_{k\in\{0,...,P\}}$. In the previous expression, $\forall i\in\{1,...,Q\}$, the basis $(\phi_k^{X_i})_{k\in\{0,...,p_{1\mathrm{D}}\}}$ is a one-dimensional polynomial basis orthonormal with respect to $\mathrm{d}\mathcal{P}_{X_i}$. When P grows, we assume it grows because the one-dimensional polynomial orders $p_{1\mathrm{D}}$ grow.

Let us assume we want to approximate a function $X\to F(X)$ such that $\int F^2(X)\,\mathrm{d}\mathcal{P}_X < \infty$. Then the P-truncated gPC expansion defined by the polynomial approximation

$$F^P(X) = \sum_{k=0}^{P} F_k\phi_k^X(X) \xrightarrow[P\to\infty]{L^2} F(X), \tag{3}$$

bears some interesting convergence properties [45, 46, 47]. Spectral convergence for F solution of the uncertain unstationary linear Boltzmann equation (1) has even been proved in [2].

Independently of the dimension or of the polynomial basis, the gPC coefficients $(F_k)_{k\in\{0,..,P\}}$ are defined by integration: they correspond to the projection of F on the components of the gPC basis with respect to the scalar product defined by $\mathrm{d}\mathcal{P}_X$:

$$F_k = \int F(X)\phi_k^X(X)\,\mathrm{d}\mathcal{P}_X, \forall k\in\mathbb{N}. \tag{4}$$

We naturally want to apply the above material to $X\to u(x,t,v,X)\ \forall x\in\mathcal{D}, \forall t\in[0,T], \forall v\in\mathcal{V}$, solution of (1). As a consequence, our aim is to compute the gPC coefficients of u by numerical integration. This can be done in practice by both non-intrusive gPC and MC-gPC:

– non-intrusive gPC [48, 49, 42, 50, 43, 51, 52] consists in introducing the set of points/weights $(X_i, w_i)_{i\in\{1,...,N\}}$ approximating random variable X and its probability measure $\mathrm{d}\mathcal{P}_X$. The

[8] Of course, simplexes such as the ones presented in [42] may be used and have less coefficients but studying their effects is beyond the scope of this paper.

[9] It is only a renumerotation.

gPC coefficients of u are consequently recovered by numerical integration: $\forall k \in \{0, ..., P\}$

$$\begin{aligned} u_k(x,t,v) &= \int_N u(x,t,v,X)\phi_k^X(X)\,\mathrm{d}\mathcal{P}_X, \\ &\approx \sum_{i=1} u(x,t,v,X_i)\phi_k^X(X_i)w_i. \end{aligned}$$

We furthermore assume that the experimental design $(X_i, w_i)_{i\in\{1,...,N\}}$ converges toward $(X,\, \mathrm{d}\mathcal{P}_X)$ in the sense that we have $\forall k \in \{0, ..., P\}$

$$u_k(x,t,v) = \int u(x,t,v,X)\phi_k^X(X)\,\mathrm{d}\mathcal{P}_X = \sum_{i=1}^{N} u(x,t,v,X_i)\phi_k^X(X_i)w_i + \mathcal{O}(N^\beta), \tag{5}$$

with $\beta < 0$. Depending on the choice of the experimental design $(X_i, w_i)_{i\in\{1,...,N\}}$, convergence can be fast or slow: for an MC experimental design, $\beta = -\frac{1}{2}$ is considered slow but is independent of the dimension Q and of the smoothness of the solution u. This is the well-known central limit theorem [29]. Gauss quadrature rules have much faster convergence rates but they strongly depends on the smoothness of the solution u and can only be applied in low to moderate dimensions [43, 44].

Independently of the choice of the experimental design, a non-intrusive application of gPC implies performing N runs of a code solving (1) in order to gather $(u(x,t,v,X_i), w_i)_{i\in\{1,...,N\}}$ and post-treat them in order to build the gPC coefficients as in (5). In our MC resolution context, each run needs N_{MC} particles such that u is approximated as $u(x,t,v,X_i) = u^{N_{MC}}(x,t,v,X_i) + \mathcal{O}(N_{MC}^{-\frac{1}{2}})$, where $u^{N_{MC}}$ is the code output. This means that we have $\forall k \in \{0, ..., P\}$

$$\begin{aligned} u_k(x,t,v) &= \sum_{i=1}^{N} u^{N_{MC}}(x,t,v,X_i)\phi_k^X(X_i)w_i + \mathcal{O}(N^\beta) + \mathcal{O}(N_{MC}^{-\frac{1}{2}}), \\ &= \sum_{i=1}^{N} u^{N_{MC}}(x,t,v,X_i)\phi_k^X(X_i)w_i + \mathcal{O}(N^\beta) + \frac{\sigma_k(x,t,v)}{\sqrt{N_{MC}}}\mathcal{G}_k. \end{aligned} \tag{6}$$

In the above expression, $(\mathcal{G}_k)_{k\in\{0,...,P\}}$ are random variables of mean zero and variance one which, at this stage, remains to be fully characterised. From the residual terms in (6), we can see that the experimental design for the uncertain variable X is tensorised with the one for the physical variables (x,t,v) with an accuracy which is $\mathcal{O}(\max(N^\beta, N_{MC}^{-\frac{1}{2}}))$. Both N and N_{MC} must grow in order to converge. MC-gPC has been introduced in [1] mainly because a full MC experimental design on the whole set of variables (x,t,v,X) can avoid this tensorization.

– MC-gPC allows integrating the gPC coefficients *on-the-fly* during MC resolution. The details are in [1] and briefly recalled in Appendix C. With MC-gPC, the gPC coefficients are computed *on-the-fly* during the MC resolution so that we have $\forall k \in \{0, ..., P\}$

$$\begin{aligned} u_k(x,t,v) &= u_k^{N_{MC}}(x,t,v) + \mathcal{O}(N_{MC}^{-\frac{1}{2}}), \\ &= u_k^{N_{MC}}(x,t,v) + \frac{\sigma_{k,\mathrm{MC}}(x,t,v)}{\sqrt{N_{MC}}}\tilde{\mathcal{G}}_k. \end{aligned} \tag{7}$$

Once again, in (7), random variables $(\tilde{\mathcal{G}}_k)_{k\in\{0,\dots,P\}}$ are of mean zero and variance one and their distributions remain to be characterised. In (7), the convergence only depends on N_{MC} which can be considered an advantage.

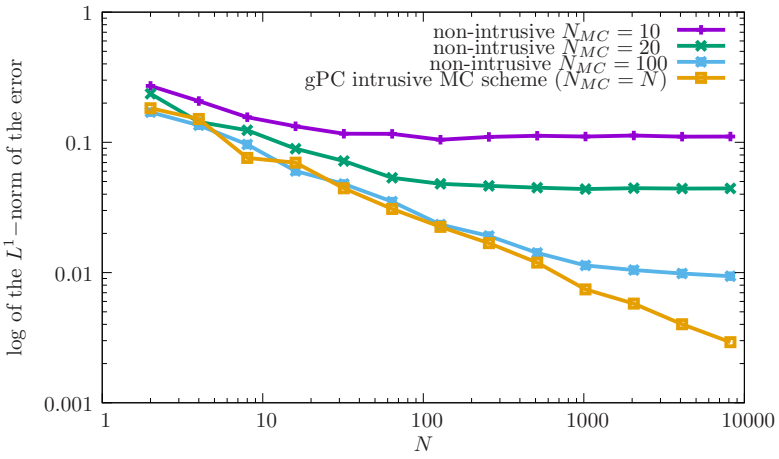

Figure 1: Convergence studies with respect to N and N_{MC} for non-intrusive gPC and MC-gPC on the variance of the number of particles.

Figure 1 illustrates the behaviours summed-up in expressions (6) and (7). It presents some convergence curves in a very simple configuration (see Appendix A for all the details) for the two above numerical methods:

- the results obtained by non-intrusive gPC use a deterministic black-box code solved by an MC scheme (the semi-analog one, see Appendix B.1) of discretisation parameter N_{MC}. The uncertain counterpart is solved with an MC sampling of $(X, \mathrm{d}\mathcal{P}_X)$ with N points. Three plots are displayed, corresponding to three convergence studies with respect to N for fixed values of $N_{MC} = 10, 20, 100$. Every curve obtained with the non-intrusive method presents, first, a converging behaviour with a slope characteristic of the numerical method used in order to integrate the uncertainties, i.e. here $\mathcal{O}(N^{-\frac{1}{2}})$. Then, the curves present a more or less pronounced kink: a change of slope, followed by a plateau, a stagnation of the accuracy. It corresponds to the point where the general accuracy becomes driven by the *coarser* numerical method, here $\mathcal{O}(N_{MC}^{-\frac{1}{2}})$. Increasing N (relative to the $x-$axis) does not allow any significant gain as $\mathcal{O}(N^{\beta}) = \mathcal{O}(N^{-\frac{1}{2}}) \ll 1$. In a sense, the locations of the kinks corresponds to optimal parameter choices (N_{MC}, N): increasing the accuracy in one direction without the other induces a loss of computational time.
- For MC-gPC, the behaviour is quite different and is described by equation (7). For MC-gPC $N = N_{MC}$, i.e. the experimental design is not anymore tensorized with the MC particles. The approximation obtained with the new MC scheme does not stagnate with the increasing number of samplings. The uncertainty is solved *on-the-fly* during the MC resolution and the convergence rate for the whole problem remains $\mathcal{O}(\frac{1}{\sqrt{N_{MC}}})$ avoiding the kinks in the curves obtained non-intrusively.

Now, from a practical point of view, if $\sigma_{k,\mathrm{MC}}$ for MC-gPC is much more important than σ_k for non-intrusive gPC, the method is not necessarily relevant and it is not clear we have a gain as much more MC particles could be needed for MC-gPC than for non-intrusive gPC. In [1, 6, 7][10], it has experimentally been verified that we probably *often* have $\sigma_k \sim \sigma_{k,\mathrm{MC}}$ so that MC-gPC does not require much more MC particles than non-intrusive gPC. *The aim of this paper is to verify it more rigorously and identify more precisely the regimes and reasons when $\sigma_k \sim \sigma_{k,MC}$ does not hold.*

In the next sections, we analytically and numerically compute σ_k and $\sigma_{k,\mathrm{MC}}$ in particular configurations and compare them. We will see that their expressions can strongly depend on the resolution scheme (non-analog, semi-analog etc.) used in the MC code or on the regimes (deterministic, uncertain, collisional etc.) involved during a simulation. For this reason, we begin, in the next section, by the numerical analysis of some (deterministic, i.e. without uncertainties) MC schemes in particular regimes.

3. Numerical noise analysis of existing Monte-Carlo schemes for (1)

As explained in several publications [1, 2, 7, 6], MC-gPC relies on few modifications of an existing MC implementation. Depending on the code, different MC schemes can be implemented (analog, implicit capture or semi-analog, non-analog etc.). We can not go through every of them so we focus on the most common ones, *the semi-analog MC scheme* (intensively used in neutronic codes) and on the non-analog MC scheme (intensively used in photonic codes). In this section, we perform the numerical analysis of their noise in a deterministic context (i.e. without uncertainties). Even in a deterministic context, the next analysis is, to our knowledge, original. It will also help performing the numerical analysis of non-intrusive gPC and of the MC-gPC schemes of section 4.

The MC schemes, semi-analog and non-analog, are recalled in Appendix B for the sake of reproducibility of the results of this paper. We insist they are commonly used and we rely on [34] for the details of their respective constructions. Both MC schemes are unbiased [29]. This means they converge toward the same result for the mean, the first moment of the particle distribution. Obviously, the schemes differ (see the different samplings and operations in Appendix B). But it is hard *a priori* having any idea of their performances. The Central Limit theorem [29] states that their performance differences can be expressed in term of convergence rate/variance[11]. We consequently study the asymptotic behaviours of the MC schemes with respect to the variance[12] of the population of particles. For this, in the next section, we rely on few simplifications: in section 3.1, we consider the free-flight regime in which every MC scheme is equivalent. In section 3.2, we consider the collisional regime in which the MC schemes can strongly differ.

3.1. The free flight regime of (1)

In this section, we consider the free flight regime. It corresponds to the particular case where $\sigma_t = \sigma_s = 0$. In this regime, the non-analog and the semi-analog MC schemes are equivalent. They

[10] This is also observable on figure 1 as the non-intrusive $N_{MC} = 100$ slope is on the same level as the one for MC-gPC.

[11] the Central Limit theorem states that the variance (if obtained from an unbiased estimator [29]) is an error estimator.

[12] and even some high order moments for the semi-analog and non-analog schemes in sections 3.2.1–3.2.2.

differ only in the collisional one, studied in section 3.2. In the deterministic free flight regime, (1) degenerates toward

$$\begin{cases} \partial_t u(x,t,v) + v\partial_x u(x,t,v) = 0, \\ u(x,0,v) = u_0(x,v), \\ u(x,t,v) = u_b(t,v), x \in \partial\mathcal{D}, \quad t \in [0,T] \quad v \cdot n_s < 0. \end{cases} \tag{8}$$

In the next sections, we study the MC resolution of equation (8). Equation (8) can be rewritten in an integral form [15]. In this case, the solution at time t is made of a contribution of the initial condition together with the the contribution of the boundary one. In order to ease the computation, let us consider an infinite medium so that (8) resumes to

$$u(x,t,v) = u_0(x - vt, v), \forall x \in \mathcal{D}, v \in \mathcal{V}, t \in [0,T]. \tag{9}$$

Let us build $\mathrm{d}u_0$ such that

$$\mathrm{d}u_0(x,v) = \frac{u_0(x,v)}{U_0}\,\mathrm{d}x\,\mathrm{d}v \text{ where } U_0(x) = \int u_0(x,v)\,\mathrm{d}v.$$

The above quantity is such that $u_0 > 0$ and sums-up to 1: it is the probability density function of the positions x and velocities v of the initial condition. Expression (9) can consequently be rewritten in an integral form as

$$\begin{aligned} u(x,t,v) &= u_0(x - vt, v), \\ &= \iint U_0 \delta_0(x - vt)\delta_0(v)\frac{u_0(x - vt, v)}{U_0}\,\mathrm{d}x\,\mathrm{d}v, \\ &= \iint U_0 \delta_0(x - vt - x_0)\delta_0(v - v_0)\,\mathrm{d}u_0(x_0, v_0). \end{aligned}$$

Introduce the random variables $\mathbf{x}_0, \mathbf{v}_0 \sim \mathrm{d}u_0(x_0, v_0)$, then the above expression can be rewritten as an expectation over path of a stochastic process as

$$u(x,t,v) \quad = \mathbb{E}\left[U_0 \delta_0(x - \mathbf{v}_0 t - \mathbf{x}_0)\delta_0(v - \mathbf{v}_0)\right],$$

where the stochastic process is given by

$$U_{x,t,v} = U_0 \delta_0(x - \mathbf{v}_0 t - \mathbf{x}_0)\delta_0(v - \mathbf{v}_0).$$

Then, by definition, we have

$$u(x,t,v) = \mathbb{E}[U_{x,t,v}].$$

The second order moment of the stochastic process $U_{x,t,v}$ is given by

$$\mathbb{E}[U^2_{x,t,v}] = \mathbb{E}[U_0^2 \delta_0(x - \mathbf{v}_0 t - \mathbf{x}_0)\delta_0(v - \mathbf{v}_0)].$$

Finally, the central limit theorem states that we have $u(x,t,v) \sim u^{N_{MC}}(x,t,v) + \frac{\sigma(x,t,v)}{\sqrt{N_{MC}}}\mathcal{G}$ with

$$\sigma(x,t,v) = \mathbb{E}[U^2_{x,t,v}] - \mathbb{E}^2[U_{x,t,v}],$$

and $\mathcal{G}$ a gaussian random variable of mean zero and variance one. In the following sections, we are going to estimate σ numerically for different values of an uncertain parameter X. The equivalent of

this quantity for non-intrusive gPC and for MC-gPC will be studied in sections 4.1.1–4.1.2 relying on the material of this section.

Let us consider an uncertain monokinetic configuration (i.e. $u(x,t,v,X) \equiv u(x,t,\omega,X)$ with $|\omega| = 1$) with initial condition given by

$$u_0(x,\omega,X) = U_0(X)\mathbf{1}_{[-x_I,x_I]}(x), x \in \mathcal{D}, X \sim \mathrm{d}\mathcal{P}_X. \tag{10}$$

The initial condition is initially isotropic with respect to the angular variable ω. In practice, we take $v = |v|\omega$ with $|v| = 1$, $x_I = 0.1$, $\mathcal{D} = [-1,1]$ and $U_0(X) = \overline{U}_0 + \hat{U}_0 X$ with $\overline{U}_0 = 1$, $\hat{U}_0 = 0.5$ with $X \sim \mathcal{U}([-1,1])$. Figure 2 (left) presents the initial spatial profiles $x \to u_0(x,X_i), i \in \{1,...,N\}$

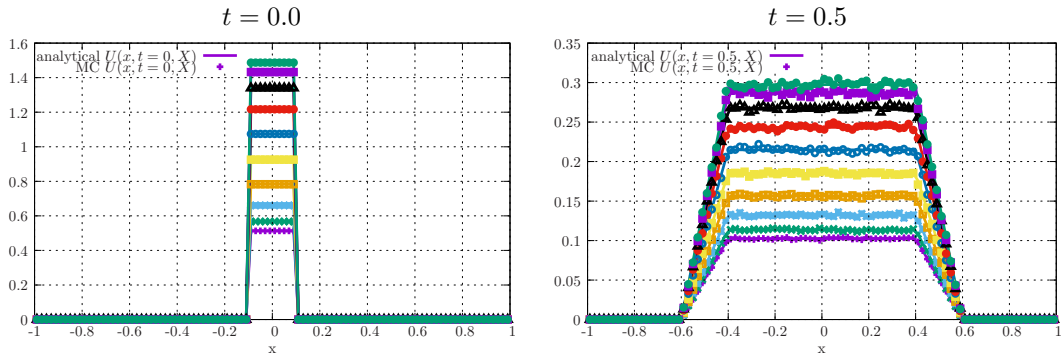

Figure 2: Spatial profiles $x \to U(x,t,X_i)$ for $i \in \{1,...,10\}$ for $t \in \{0.0, 0.5\}$ from the analytical solutions and from MC ones.

for $N = 10$ Gauss-Legendre points and $N_x = 100$ cells. The uncertainty only affects the plateaus of the initial conditions. Figure 2 (right) presents both the analytical solutions

$$\begin{aligned} u(x,t,X) &= \int u(x,t,\omega,X)\,\mathrm{d}\omega = \int u_0(x-\omega t,\omega,X)\,\mathrm{d}\omega, \\ &= U_0(X)\int_{-1}^{1} \mathbf{1}_{[-x_I,x_I]}(x-\omega t)\frac{1}{2}\,\mathrm{d}\omega, \end{aligned} \tag{11}$$

at the $N = 10$ Gauss-Legendre points and the corresponding numerical results obtained from an MC code: on figure 2 (right), the results are in good agreement despite the numerical noise of the MC code. Now, our aim is mainly to study the amplitude of this numerical MC noise: figure 3 presents the numerical approximations of the spatial profiles $x \to \sigma(x,t,X_i), i \in \{1,...,N\}$ obtained by two different ways:

- first, thanks to the MC estimator instrumenting every MC resolution (the computations used $N_{MC} = 5 \times 10^4$),
- Second, thanks to an estimation relying on $N_{\text{seed}} = 1000$ runs with $N_{MC} = 100$ particles, each initialised with a different seed and by evaluating the second order moment of random variable $(u(x,t,X) - \mathbb{E}[U_{x,t}](X))\sqrt{N_{MC}}$, i.e.

$$t \to \mathbb{V}\left[(u(x,t,X) - \mathbb{E}[U_{x,t}](X))\sqrt{N_{MC}}\right], \tag{12}$$

where $u(x,t,X)$ is the analytical solution given by (11). According to the Central Limit Theorem (and due to the unbiasedness of the estimator used in the MC code) we have[13] $(u(x,t,X) - \mathbb{E}[U_{x,t}](X))\sqrt{N_{MC}} \sim \mathcal{G}(0, \sigma(x,t,X))$.

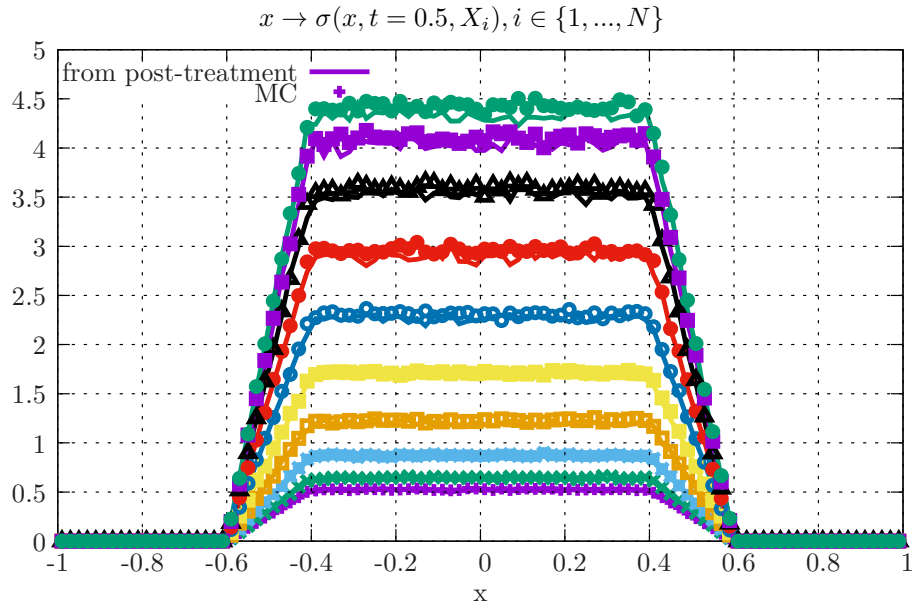

Figure 3: Spatial profiles $x \to \sigma(x, t = 0.5, X_i)$ for $i \in \{1, ..., N = 10\}$ Gauss-Legendre points for $t = 0.5$. The results are obtained from two different ways: the curves labeled 'from post-treatement' are estimated by using the analytical solution (11) in (12). The dotted 'MC' curves are obtained from the MC estimators of the code.

In figure 3, the spatial errors for every $(X_i)_{i\in\{1,...,N=10\}}$ obtained using the analytical solution (11) in (12) are in agreement with the variances computed during the MC resolutions. These numerical experiments allow verifying our developments (see V&V [41]). The analysis will consequently be used in section 4.1.1 in order to compute the variances $(\sigma_k^2)_{k\in\{0,...,P\}}$ on the gPC coefficients obtained non-intrusively.

3.2. The collisional regime for (1)

Let us now consider the collisional regime. For this, we assume we are in a *monokinetic homogeneous configuration*. It corresponds to the case of an infinite medium with constant cross-sections with respect to time, space and energy. With these assumptions, the transport equation (1) resumes to

$$\partial_t \int u(t,\omega,X)\,\mathrm{d}\omega + v\sigma_t(X)\int u(t,\omega,X)\,\mathrm{d}\omega = \sigma_s(X)\int vP_s(\omega',\omega,X)u(t,\omega',X)\,\mathrm{d}\omega'. \tag{13}$$

[13] where $\mathcal{G}(\mu,\sigma)$ denotes a gaussian random variable of mean μ and variance σ^2.

From the definition of P_s ensuring[14] $\forall \omega \in \mathbb{S}^2, \forall X \in \Omega, \int P_s(\omega', \omega, X)\,\mathrm{d}\omega' = 1$, it even simplifies to the classical ODE

$$\partial_t U(t,X) + v\sigma_t(X)U(t,X) = v\sigma_s(X)U(t,X).$$

Its solution is $U(t,X) = U_0(X)e^{-v(\sigma_t(X)-\sigma_s(X))t}$ where $U(t,X) = \int u(t,\omega,X)\,\mathrm{d}\omega$. In the following sections, we verify the two MC schemes (semi- and non-analog) are converging for the mean solution (i.e. unbiased). We furthermore compute their asymptotical higher order moments. The latters allow comparing their performances *via* the analytical expression of their asymptotical variances.

3.2.1. Asymptotic mean and variance of the semi-analog scheme

The starting point of the analysis is the expectation form of the transport equation (B.6) for the semi-analog MC scheme with the monokinetic, homogenous and deterministic assumptions (i.e. $\sigma_\alpha(x,v,X) \equiv \sigma_\alpha, \forall \alpha \in \{s,t\}$ and $u(x,t,v,X) \equiv u(t,\omega)$). With these assumptions, the recursive equation (B.6) becomes

$$U(t) = \mathbb{E}\left[\mathbf{1}_{[t,\infty[}(\tau)U_0 + \mathbf{1}_{[0,t]}(\tau)\frac{\sigma_s}{\sigma_t}U(t-\tau)\right]. \tag{14}$$

In the above expression, we have $\tau \sim \mathcal{E}(v\sigma_t)$ which must be read τ *is an exponential random variable of parameter* $v\sigma_t$. We suggest expanding the recursive part into an infinite sum over the number of interactions. Let us introduce a new random variable $S_i = \sum_{k=0}^{i}\tau_k$ where $\tau_k \sim \mathcal{E}(v\sigma_t)$ $\forall k \in \{1,...,i\}$ are independent identically distributed. Random variable S_i follows a Gamma law of parameters $(v\sigma_t, i)$, denoted by $S_i \sim \Gamma(v\sigma_t, i)$. Let us introduce U_t the stochastic process induced by the possible histories of any MC particles. It is given by

$$U_t = \sum_{k=0}^{\infty}\mathbf{1}_{[0,t]}(S_k)\mathbf{1}_{[t,\infty[}(S_k+\tau_{k+1})\left(\frac{\sigma_s}{\sigma_t}\right)^k U_0.$$

The indice k denotes the number of interactions encountered by any MC particles for times in $[0,t]$. The indicatrices

$$\mathbf{1}_{[0,t]}(S_k)\mathbf{1}_{[t,\infty[}(S_k+\tau_{k+1}),$$

express the fact an MC particle encounters exactly k interactions for times between $[0,t]$. The first moment is defined by $U(t) = \mathbb{E}[U_t]$, and by linearity its expression becomes

$$\begin{aligned} U(t) &= \mathbb{E}\left[U_t\right] = \mathbb{E}\left[\sum_{k=0}^{\infty}\mathbf{1}_{[0,t]}(S_k)\mathbf{1}_{[t,\infty[}(S_k+\tau_{k+1})\left(\frac{\sigma_s}{\sigma_t}\right)^k U_0\right], \\ &= U_0\sum_{k=0}^{\infty}\mathbb{E}\left[\mathbf{1}_{[0,t]}(S_k)\mathbf{1}_{[t,\infty[}(S_k+\tau_{k+1})\right]\left(\frac{\sigma_s}{\sigma_t}\right)^k, \\ &= U_0\sum_{k=0}^{\infty}\mathbb{P}\left(\tau_{k+1} > t - S_k | S_k < t\right)\left(\frac{\sigma_s}{\sigma_t}\right)^k. \end{aligned} \tag{15}$$

Replacing the probability of having k interactions by its expression

$$\mathbb{P}\left(\tau_{k+1} > t - S_k | S_k < t\right) = e^{-v\sigma_t t}(v\sigma_t)^k\frac{s^k}{k!}, \tag{16}$$

[14] It only corresponds to a pretreatment of the cross-sections.

leads to

$$\begin{aligned} U(t) &= U_0 \sum_{k=0}^{\infty} e^{-v\sigma_t t}(v\sigma_t)^k \frac{s^k}{k!} \left(\frac{v\sigma_s}{v\sigma_t}\right)^k, \\ &= U_0 e^{-v\sigma_t t} \sum_{k=0}^{\infty} (v\sigma_s)^k \frac{s^k}{k!}, \\ &= U_0 e^{-v(\sigma_t-\sigma_s)t}. \end{aligned} \tag{17}$$

With the few previous computations, we formally verified the semi-analog MC scheme is unbiased. Let us now study the moment of order M of the stochastic process U_t. It is defined as $\mathbb{E}\left[U_t^M\right]$ with

$$U_t^M = U_0^M \sum_{i_1=0}^{\infty} ... \sum_{i_M=0}^{\infty} \mathbf{1}_{[0,t]}(S_{i_1})\mathbf{1}_{[t,\infty[}(S_{i_1}+\tau_{i_1+1})...\mathbf{1}_{[0,t]}(S_{i_M})\mathbf{1}_{[t,\infty[}(S_{i_M}+\tau_{i_M+1}) \left(\frac{\sigma_s}{\sigma_t}\right)^{i_1+...+i_M}.$$

In the previous expression, we expanded the exponant M into M summations over indices $(i_1, ..., i_M)$. Using the generalization to M terms of the fact that $\forall (k,m) \in \mathbb{N}^2$, we have

$$\mathbf{1}_{[0,t]}(S_k)\mathbf{1}_{[t,\infty[}(S_k+\tau_{k+1})\mathbf{1}_{[0,t]}(S_m)\mathbf{1}_{[t,\infty[}(S_m+\tau_{m+1}) = \delta_{k,m}\mathbf{1}_{[0,t]}(S_m)\mathbf{1}_{[t,\infty[}(S_m+\tau_{m+1}).$$

We can then simplify the above expression of U_t^M into

$$U_t^M = U_0^M \sum_{i=0}^{\infty} \mathbf{1}_{[0,t]}(S_i)\mathbf{1}_{[t,\infty[}(S_i+\tau_{i+1}) \left(\frac{\sigma_s}{\sigma_t}\right)^{M\times i}.$$

Taking the expectation of U_t^M leads to

$$\begin{aligned} \mathbb{E}[U_t^M] &= U_0^M \sum_{i=0}^{\infty} \mathbb{P}\left(\tau_{i+1} > t - S_i | S_i < t\right) \left(\frac{\sigma_s}{\sigma_t}\right)^{M\times i}, \\ &= U_0^M e^{-v\sigma_t t} \sum_{i=0}^{\infty} (v\sigma_t)^i \frac{t^i}{i!} \left(\frac{\sigma_s}{\sigma_t}\right)^{M\times i}, \\ &= U_0^M \exp\left(\frac{(v\sigma_s)^M - (v\sigma_t)^M}{(v\sigma_t)^{M-1}} t\right). \end{aligned} \tag{18}$$

The latter expression is in agreement with the moment of order 1 and allows obtaining the asymptotic variance (*via* $\mathbb{E}[U_t]$ and $\mathbb{E}[U_t^2]$) of the homogeneous process U_t for the semi-analog scheme:

$$\begin{aligned} \sigma_{\text{sa}}^2(t) &= \mathbb{E}[U_t^2] - \left(\mathbb{E}[U_t]\right)^2, \\ &= U_0^2 \left(e^{\dfrac{(v\sigma_s)^2 - (v\sigma_t)^2}{(v\sigma_t)} t} - e^{2(v\sigma_s - v\sigma_t)t} \right). \end{aligned} \tag{19}$$

To our knowledge, expression (19) has never been stated and the above (deterministic) result is original. Let us now verify, see verification & validation (V&V [41]), our analysis. Figure 4 compares the results obtained with

– the analytical expression (18) for several orders for the moments $(\mathbb{E}[U_t^M])_{M\in\{1,2,3,4\}}$,

– and an instrumentation of an MC code in which the semi-analog MC scheme is implemented and in which $(\mathbb{E}[U_t^M])_{M\in\{1,2,3,4\}}$ is estimated within the MC tracking.

The comparisons are made for two different configurations,

– an absorbing one (figure 4 left), with

$$U_0 = 1, \sigma_t = 1.00, \sigma_s = 0.85, v = 1, \tag{20}$$

– and a multiplicative one (figure 4 right), with

$$U_0 = 1, \sigma_t = 1.00, \sigma_s = 1.01, v = 1. \tag{21}$$

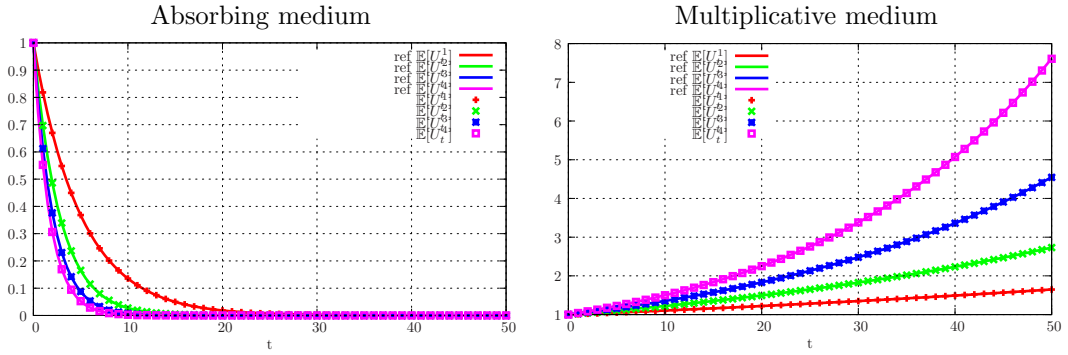

Figure 4: Time evolutions of the moments $t \to \mathbb{E}[U_t^n]$ for $n \in \{1, 2, 3, 4\}$ in the absorbing (20) and multiplicative (21) configurations.

First, depending on the configuration (absorbing or multiplicative), the moments are either (respectively) decreasing fast (figure 4 left) or growing fast (figure 4 right). Independently of the configuration, the high order moments numerically estimated are in very good agreement with the analytical ones given by (18).

The high order moments have an interest in terms of V&V [41]. But we are mainly interested in the second order moment $\mathbb{E}[U_t^2]$ used to compute the variance (19). Figure 5 (top) compares

– the time evolution of the analytical variance (19),

– the time evolution of the variance estimated during the semi-analog MC resolution (the computation used $N_{MC} = 5 \times 10^4$),

– the time evolution of the variance estimated by relying on $N_{\text{seed}} = 1000$ runs with $N_{MC} = 100$ particles, each initialised with a different seed and by evaluating the variance of the random variable $(U(t) - \mathbb{E}[U_t])\sqrt{N_{MC}}$, i.e.

$$t \to \mathbb{V}\left[(U(t) - \mathbb{E}[U_t])\sqrt{N_{MC}}\right]. \tag{22}$$

According to the Central Limit Theorem (and due to the unbiasedness of the semi-analog estimator) we have[15] $(U(t) - \mathbb{E}[U_t])\sqrt{N_{MC}} \sim \mathcal{G}(0, \sigma_{\text{sa}}(t))$.

[15] where $\mathcal{G}(\mu, \sigma)$ denotes a gaussian random variable of mean μ and variance σ^2.

The comparisons are made on the two previously described situations (20) and (21) in figure 5 (top). In the absorbing situation, the error with respect to time has a maximum around $t \approx 3$ and

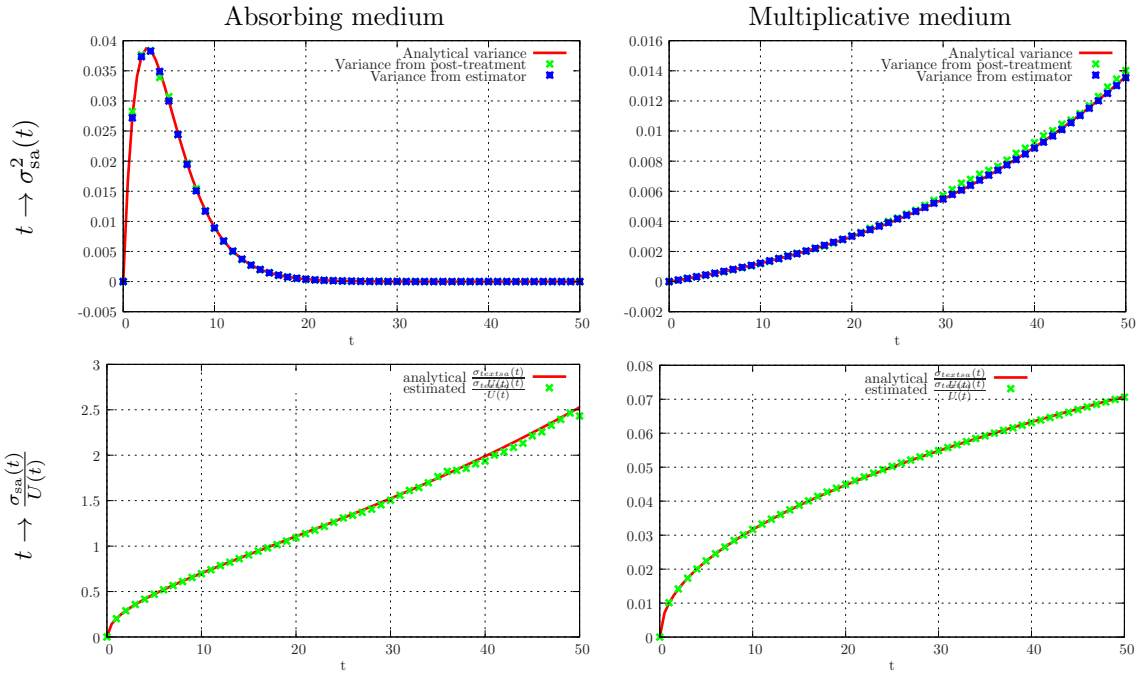

Figure 5: Top: time evolutions $t \to \sigma^2_{\rm sa}(t)$ (analytical variance), $t \to \mathbb{V}[U^n_t]$ and (12) in the absorbing (20) and multiplicative (21) configurations. Bottom: time evolutions $t \to \frac{\sigma_{\rm sa}(t)}{U(t)}$ (analytical and estimated thanks to the instrumentaion of the MC code) in the absorbing (20) and multiplicative (21) configurations.

decreases as the population of particle dies out. On another hand, for the multiplicative case, the error explodes just as the population of particle explodes. The time evolutions of the ratio *standard deviation over mean*, i.e $t \to \frac{\sigma_{\rm sa}(t)}{U(t)}$ are also displayed in figure 5 (bottom) in both configurations (20) and (21). This ratio grows linearly with time as the population of particles dies out (see figure 5 top-left) whereas this ratio remains way smaller in the multiplicative case (see figure 5 bottom-right). This means that the relative accuracy is better in the multiplicative situation here (of course, this ratio needs to be divided by $\sqrt{N_{MC}}$ in order to give an idea of the relative error). Besides, as the population dies out, it is well known the linear Boltzmann equation is not an accurate enough model and one needs to rely on more complex ones [53, 54, 55].

From figure 5, we verify our analysis of the moments for the semi-analog MC scheme: the numerical results (obtained by several different ways) are in agreement with the analytical expression (19), independently of the time, the values of the cross-sections or the initial condition.

Let us now develop the same computations for the non-analog scheme before considering uncertain problems in section 4.

3.2.2. Asymptotic mean and variance of the non-analog scheme

Let us apply the same methodology to the non-analog MC scheme and compute the M^{th} order moments of any non-analog MC solution of (13). For this, we come back to the expectation form of the transport equation from which the MC scheme is built. With the assumptions detailed above, the recursive equation (B.13) becomes

$$U(t) = \mathbb{E}\left[\mathbf{1}_{[t,\infty[}(\tau)U_0 e^{-v\sigma_a t} + \mathbf{1}_{[0,t]}(\tau)e^{-v\sigma_a(t-\tau)}U(t-\tau)\right], \tag{23}$$

with $\sigma_a = \sigma_t - \sigma_s$. We recall $\tau \sim \mathcal{E}(v\sigma_s)$. Let us expand the recursive part into an infinite sum over the number of interactions thanks to $S_i = \sum_{k=0}^{i} \tau_k$ where $\tau_k \sim \mathcal{E}(v\sigma_s)\ \forall k \in \{1, ..., i\}$ are independent identically distributed. Random variable S_i follows a Gamma law of parameters $(v\sigma_s, i)$, denoted by $S_i \sim \Gamma(v\sigma_s, i)$. Then (B.15), the equation for the mean (or the moment of order 1) rewrites

$$\begin{aligned} U(t) &= \mathbb{E}\left[U_t\right] = \mathbb{E}\left[\sum_{k=0}^{\infty} \mathbf{1}_{[0,t]}(S_k)\mathbf{1}_{[t,\infty[}(S_k + \tau_{k+1})e^{-v\sigma_a t_{k+1}}U_0\right], \\ &= U_0 e^{-v\sigma_a t}\underbrace{\sum_{k=0}^{\infty} \mathbb{P}\left(\tau_{k+1} > t - S_k | S_k < t\right)}_{=1}, \\ &= U_0 e^{-v\sigma_a t}. \end{aligned} \tag{24}$$

We then recover the analytical solution of the homogeneous problem and formally verified that the non-analog scheme is unbiased. Note that in this homogeneous configuration, the convergence of the non-analog scheme does not even depend on the probability measure of the interaction times τ_k, S_k as the sum over k always equals 1, whatever this choice. The interesting part concerns the moments of higher orders. Their computations are in fact very similar to the previous one. Few computations lead to expression

$$\mathbb{E}[U_t^M] = U_0^M e^{-Mv\sigma_a t}. \tag{25}$$

The latter expression is in agreement with the moment of order 1 and allows showing the asymptotic variance of the homogeneous process for the non-analog scheme is given by:

$$\sigma^2_{\text{na}}(t) = 0. \tag{26}$$

This property of the non-analog scheme is singular: the zero variance result (26) allows recovering the fact that in the homogenous case, only one MC particle is enough for the non-analog MC scheme to restitute the analytical solution. For this scheme, we do not plot the curves as they are all equal to zero except for the first moment $t \to U(t) = \mathbb{E}[U_t]$ but we ensure we numerically recover analytical expressions (25) and (26) in the same conditions as in the previous section 3.2.1.

4. Numerical noise analysis of existing uncertain Monte-Carlo schemes for (1)

In this section, we compute the variances of two stochastic (i.e. with uncertainties) MC schemes in the free-flight regime and in the collisional one. Each section begins by the study of the variances of the gPC coefficients of a non-intrusive application of gPC [48, 49, 42, 50, 43, 51, 52]. In section 4.1, we focus on the uncertain free-flight regime and in sections 4.2–4.3 on the uncertain collisional one. The sections end with the study of the variances of the coefficients obtained by MC-gPC and their comparisons with the ones obtained with non-intrusive gPC.

4.1. Non-intrusive gPC and MC-gPC for the uncertain free-flight regime

We study the uncertain free-flight regime with non-intrusive gPC in section 4.1.1 and with MC-gPC in section 4.1.2. In particular, the asymptotical variances $(\sigma_k^2)_{k\in\{0,...,P\}}$ and $(\sigma_{k,\mathrm{MC}}^2)_{k\in\{0,...,P\}}$ of expressions (6) and (7) are estimated and compared in this regime.

4.1.1. The non-intrusive gPC resolution of the uncertain free-flight regime

The gPC coefficients, by definition see [48, 49, 42, 50, 43, 51, 52], are given by $\forall k \in \{0, ..., P\}$

$$u_k(x,t,v) = \int u(x,t,v,X)\phi_k(X)\,\mathrm{d}\mathcal{P}_X.$$

Besides, from section 3, we know that once u is approximated with an MC resolution scheme, we have

$$u^{N_{MC}}(x,t,v,X) = u(x,t,v,X) + \frac{\sigma(x,t,v,X)}{\sqrt{N_{MC}}}\mathcal{G}(X),$$

where $\mathcal{G}(X)$ is a white noise indexed by X of mean zero and variance one. Note that it is a white noise (i.e. uncorrelated) because for each X, every MC simulations are independent. The asymptotic mean of $u^{N_{MC}}$ is u and its asymptotic standard deviation is $\frac{\sigma}{\sqrt{N_{MC}}}$.

From the last equation, we want to obtain the asymptotical mean and variance of the approximated gPC coefficients $(u_k^{N_{MC}})_{k\in\{0,...,P\}}$. We need to study the mean and variance of

$$\begin{aligned} u_k^{N_{MC}}(x,t,v) &= \int u^{N_{MC}}(x,t,v,X)\phi_k(X)\,\mathrm{d}\mathcal{P}_X, \\ &= \int \left[u(x,t,v,X) + \frac{\sigma(x,t,v,X)}{\sqrt{N_{MC}}}\mathcal{G}(X)\right]\phi_k(X)\,\mathrm{d}\mathcal{P}_X, \forall k \in \{0,...,P\}. \end{aligned} \tag{27}$$

Let us begin with the mean: taking the expectation of (27) and interchanging the expectation and the integral leads to $\forall k \in \{0, ..., P\}$

$$\begin{aligned} \mathbb{E}\left[u_k^{N_{MC}}(x,t,v)\right] &= \int \mathbb{E}\left[u(x,t,v,X) + \frac{\sigma(x,t,v,X)}{\sqrt{N_{MC}}}\mathcal{G}(X)\right]\phi_k(X)\,\mathrm{d}\mathcal{P}_X, \\ &= \int u(x,t,v,X)\phi_k(X)\,\mathrm{d}\mathcal{P}_X, \\ &= u_k(x,t,v). \end{aligned} \tag{28}$$

The above expression ensures the estimation of the gPC coefficients is unbiased. In order to compute the asymptotic variance, we need first to compute the second order moment of $(u_k^{N_{MC}})_{k\in\{0,...,P\}}$:

$$\begin{aligned} &\mathbb{E}\left[\left(u_k^{N_{MC}}(x,t,v)\right)^2\right] \\ &= \mathbb{E}\left[\left(\int\left[u(x,t,v,X) + \frac{\sigma(x,t,v,X)}{\sqrt{N_{MC}}}\mathcal{G}(X)\right]\phi_k(X)\,\mathrm{d}\mathcal{P}_X\right)^2\right], \\ &= \mathbb{E}\left[\int\left[u(x,t,v,X) + \frac{\sigma(x,t,v,X)}{\sqrt{N_{MC}}}\mathcal{G}(X)\right]\phi_k(X)\,\mathrm{d}\mathcal{P}_X\int\left[u(x,t,v,Y) + \frac{\sigma(x,t,v,Y)}{\sqrt{N_{MC}}}\mathcal{G}(Y)\right]\phi_k(Y)\,\mathrm{d}\mathcal{P}_X\right], \\ &= \mathbb{E}\left[\iint\left[u(x,t,v,X) + \frac{\sigma(x,t,v,X)}{\sqrt{N_{MC}}}\mathcal{G}(X)\right]\left[u(x,t,v,Y) + \frac{\sigma(x,t,v,Y)}{\sqrt{N_{MC}}}\mathcal{G}(Y)\right]\phi_k(X)\phi_k(Y)\,\mathrm{d}\mathcal{P}_X(X)\,\mathrm{d}\mathcal{P}_X(Y)\right]. \end{aligned} \tag{29}$$

Let us now interchange the expectation and the integral, just as in the previous calculation for the mean, in order to obtain:

$$\begin{aligned}&\mathbb{E}\left[\left(u_k^{N_{MC}}(x,t,v)\right)^2\right] = \\ &\iint \mathbb{E}\left[\left(u(x,t,v,X)+\frac{\sigma(x,t,v,X)}{\sqrt{N_{MC}}}\mathcal{G}(X)\right)\left(u(x,t,v,Y)+\frac{\sigma(x,t,v,Y)}{\sqrt{N_{MC}}}\mathcal{G}(Y)\right)\right]\phi_k(X)\phi_k(Y)\,\mathrm{d}\mathcal{P}_X(X)\,\mathrm{d}\mathcal{P}_X(Y).\end{aligned} \tag{30}$$

Due to the fact that $\mathcal{G}(X)$ and $\mathcal{G}(Y)$ are uncorrelated, we finally get

$$\mathbb{E}\left[\left(u_k^{N_{MC}}(x,t,v)\right)^2\right] = u_k^2(x,t,v,X)+\int\frac{\sigma^2(x,t,v,X)}{N_{MC}}\phi_k(X)\,\mathrm{d}\mathcal{P}_X, \tag{31}$$

so that the asymptotic variance of the gPC coefficients is given, $\forall k\in\{0,...,P\}$, by

$$\mathbb{V}\left[\left(u_k^{N_{MC}}(x,t,v)\right)^2\right] = \int\frac{\sigma^2(x,t,v,X)}{N_{MC}}\phi_k(X)\,\mathrm{d}\mathcal{P}_X. \tag{32}$$

Its asymptotic standard deviation is consequently given by

$$\sqrt{\mathbb{V}}\left[\left(u_k^{N_{MC}}(x,t,v)\right)^2\right] = \frac{1}{\sqrt{N_{MC}}}\sqrt{\int\sigma^2(x,t,v,X)\phi_k(X)\,\mathrm{d}\mathcal{P}_X}. \tag{33}$$

The numerical error on the gPC coefficients computed non-intrusively can consequently be estimated thanks to the experimental design $(X_i,w_i)_{i\in\{1,...,N\}}\sim(X,\,\mathrm{d}\mathcal{P}_X)$ *via* expression

$$\begin{aligned}\sigma_k^2(x,t,v) &= \int\frac{\sigma^2(x,t,v,X)}{N_{MC}}\phi_k(X)\,\mathrm{d}\mathcal{P}_X,\\ &= \sum_{i=1}^{N}\frac{\sigma^2(x,t,v,X_i)}{N_{MC}}\phi_k(X_i)w_i+\mathcal{O}(N^\beta).\end{aligned} \tag{34}$$

In the next paragraphs, we consider a particular configuration, estimate the above variances/errors and verify our analysis before performing a similar one on the MC-gPC estimated coefficients. Note that care is taken to make sure we have $\mathcal{O}(N^\beta)\ll 1$ in order to avoid confusing results.

Figure 7 (left) presents the spatial profiles of the gPC coefficients $x\to u_k(x,t=0.5)$ for $k\in\{0,..P=4\}$ obtained by numerically integrating the analytical solution (11) and the outputs of the MC code. First, the results are in agreements, with an observable MC noise. For this test-case, u_0,u_1 and u_2 are non-zero (even if u_2 is small). We can see in figure 7 (left) that the numerical MC noise for u_3 and u_4 fluctuates around zero: this testifies of a fast convergence with respect to the polynomial order P (see [2]). Figure 7 (right) presents the spatial profiles $x\to\sigma_k^2(x,t=0.5)$ for $k\in\{0,...,P=4\}$ in the same configuration as before. The numerical MC noise is higher on the first coefficients u_0 and decreases for the successive orders. The asymptotical variances for u_3 and u_4 (which are close to zero) are very small.

4.1.2. The MC-gPC resolution of the uncertain free-flight regime

Let us now perform the same analysis but for the numerical MC noise obtained from an MC-gPC resolution. In an infinite medium, in the same conditions as in the previous section, we have $\forall k\in\{0,...,P\}$

$$u_k(x,t,v)=\int u_0(x-vt,v,X)\phi_k(X)\,\mathrm{d}\mathcal{P}_X. \tag{35}$$

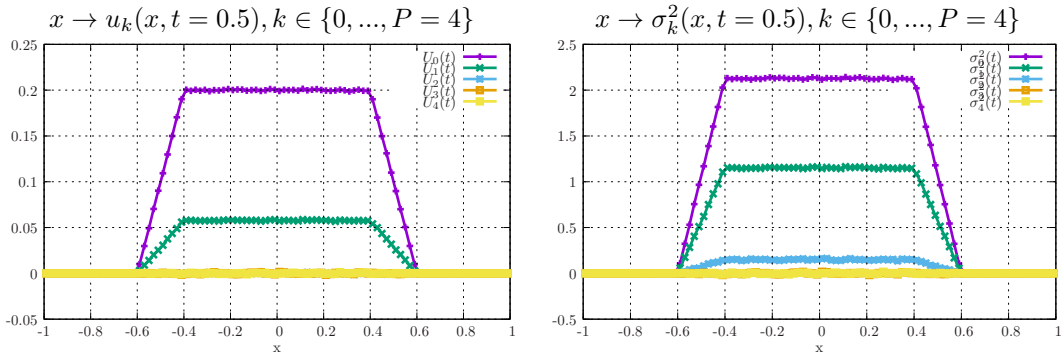

Figure 6: Spatial profiles of the gPC coefficients $x \to u_k(x, t = 0.5)$ for $k \in \{0, ..., P = 4\}$ (left) and of the variances of the gPC coefficients $x \to \sigma_k(x, t = 0.5)$ for $k \in \{0, ..., P = 4\}$ both obtained thanks to non-intrusive gPC.

MC-gPC consists in taking X into account within the MC scheme in the early stages of the resolution. For example, it consists in building $\mathrm{d}u_0$ such that

$$\mathrm{d}u_0(x, v, X) = \frac{u_0(x, v, X)}{U_0(X)} \,\mathrm{d}x\,\mathrm{d}v \text{ where } U_0(X) = \iint u_0(x, v, X)\,\mathrm{d}x\,\mathrm{d}v.$$

The above quantity is such that $u_0 > 0$ and sums-up to 1 $\forall X \sim \mathrm{d}\mathcal{P}_X$: it is the probability density function of the positions x and velocities v of the initial condition with uncertainty $X \sim \mathrm{d}\mathcal{P}_X$. Expression (35) can consequently be rewritten as an expectation as

$$\begin{aligned} u_k(x, t, v) &= \int u_0(x - vt, v, X)\phi_k(X)\,\mathrm{d}\mathcal{P}_X, \\ &= \iiint U_0(X)\delta_0(x - vt - x_0)\delta_0(v - v_0)\frac{u_0(x_0, v_0, X)}{U_0(X)}\,\mathrm{d}x_0\,\mathrm{d}v_0\phi_k(X)\,\mathrm{d}\mathcal{P}_X, \\ &= \iiint U_0(X)\delta_0(x - vt - x_0)\delta_0(v - v_0)\phi_k(X)\,\mathrm{d}u_0(x_0, v_0, X)\,\mathrm{d}\mathcal{P}_X. \end{aligned}$$

Introduce the random variables $\mathbf{X}_0 \sim \mathrm{d}\mathcal{P}_X$ and $\mathbf{x}_0, \mathbf{v}_0 \sim \mathrm{d}u_0(x_0, v_0, \mathbf{X}_0)$, then the above expression can be rewritten

$$u_k(x, t, v) = \mathbb{E}\left[U_0(\mathbf{X}_0)\delta_0(x - \mathbf{v}_0 t - \mathbf{x}_0^X)\delta_0(v - \mathbf{v}_0)\phi_k(\mathbf{X}_0)\right].$$

Let us introduce

$$U_{x,t,v,k} = U_0(\mathbf{X}_0)\delta_0(x - \mathbf{v}_0 t - \mathbf{x}_0)\delta_0(v - \mathbf{v}_0)\phi_k(\mathbf{X}_0).$$

Then, we have by definition

$$u_k(x, t, v) = \mathbb{E}[U_{x,t,v,k}].$$

The second order moment of the stochastic process $U_{x,t,v,k}$ is given by

$$\mathbb{E}[U_{x,t,v,k}^2] = \mathbb{E}[U_0^2(\mathbf{X}_0)\delta_0(x - \mathbf{v}_0 t - \mathbf{x}_0)\delta_0(v - \mathbf{v}_0)\phi_k^2(\mathbf{X}_0)],$$

and can be estimated in order to approximate the variance $(\sigma_{k,\mathrm{MC}}^2)_{k\in\{0,...,P\}}$ of the MC-gPC estimators on the gPC coefficients $(u_k)_{k\in\{0,...,P\}}$:

$$\sigma_{k,\mathrm{MC}}^2(x, t, v) = \mathbb{E}[U_{x,t,v,k}^2] - \mathbb{E}^2[U_{x,t,v,k}].$$

Figure 7 (left) compares the the gPC coefficients $(u_k)_{k\in\{0,...,P\}}$ approximated with non-intrusive gPC and MC-gPC with the same number of N_{MC} of MC particles. The non-intrusive runs used $N = 30$ (in order to make sure $\mathcal{O}(N^\beta) \ll 1$). The two resolution schemes give satisfactory results on every gPC coefficients. On figure 7 (left), we can emit the hypothesis that the MC-gPC coefficients

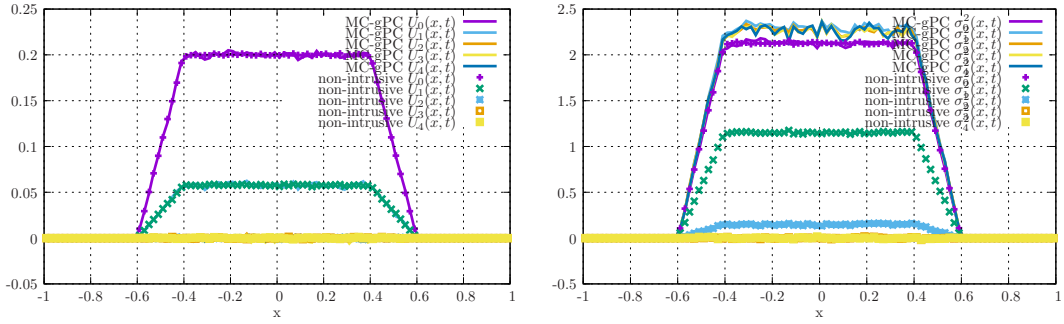

Figure 7: Left: spatial profiles $x \to U_k(x,t)$ for $k \in \{0,...P = 4\}$ for $t = 0.5$ obtained from non-intrusive gPC and MC-gPC. Right: spatial profiles $x \to \sigma^2_{k,\mathrm{MC}}(x,t)$ for $k \in \{0,...P = 4\}$ for $t = 0.5$ obtained from non-intrusive gPC and MC-gPC.

are a little bit noiser than the non-intrusive ones. This can be verified by computing the variances $(\sigma^2_{k,\mathrm{MC}})_{k\in\{0,...,P\}}$ of the different estimators, see figure 7 (right). First, the variances of the first coefficients u_0 are the same for non-intrusive gPC and MC-gPC: the two resolution schemes seem to have the same performances on the mean u_0. On another hand, the variances on coefficient u_1 is 2 times more important for MC-gPC than for non-intrusive gPC which tends to confirm the observation on figure 7 (left). In fact, with MC-gPC, the variances on all coefficients for $k > 1$ seem to be equivalent whereas they tend to decrease for non-intrusive gPC.

In this regime, we can observe that MC-gPC is a little bit noisier than non-intrusive gPC. But it remains hard identifying the reason why this increase of variance occurs. In the next sections, by considering the collisional regime and by obtaining analytical expressions of the different variances, we are going to be able to go further in the analysis and identify the term which is responsible for this increase of variance for MC-gPC.

4.2. Non-intrusive semi- and non-analog MC schemes in the collisional regime

In this section, we exhibit the analytical variances we obtain by applying non-intrusive gPC in the collisional regime. The projection of the solution u on the components of the basis are given by

$$u_k(x,t,v) = \int u(x,t,v,X)\phi_k(X)\,\mathrm{d}\mathcal{P}_X, \forall k \in \{0,...,P\}.$$

In the numerical examples of the following sections, as we focus on the collisional regime, we are in the monokinetic homogenous context and the above expression resumes to

$$U_k(t) = \int U(t,X)\phi_k(X)\,\mathrm{d}\mathcal{P}_X, \forall k \in \{0,...,P\},$$

where the solution $U(t,X)$ of the *uncertain* monokinetic homogeneous equation (1) is given by $\forall X \sim \mathrm{d}\mathcal{P}_X$

$$U(t,X) = U_0(X) e^{-v(\sigma_t(X)-\sigma_s(X))t}. \tag{36}$$

In the two next sections, we study the non-intrusive gPC resolution on an MC code in which

– the semi-analog MC scheme is implemented, see section 4.2.1,

– the non-analog MC scheme is implemented, see section 4.2.2.

4.2.1. Non-intrusive semi-analog MC schemes in the collisional regime

From (19), the variance of the error made $\forall X \in \mathrm{d}\mathcal{P}_X$ in a non-intrusive resolution is

$$\sigma^2_{\mathrm{sa}}(t,X) = U_0^2(X) \left(e^{\dfrac{(v\sigma_s(X))^2 - (v\sigma_t(X))^2}{(v\sigma_t(X))} t} - e^{2(v\sigma_s(X)-v\sigma_t(X))t} \right). \tag{37}$$

As a consequence, asymptotically with N_{MC}, according to the Central Limit Theorem, the error made on $U(t,X)$, $\forall X \in \mathrm{d}\mathcal{P}_X$ is given by

$$U(t,X) - U^{N_{MC}}(t,X) \sim \mathcal{G}\left(0, \frac{\sigma_{\mathrm{sa}}(t,X)}{\sqrt{N_{MC}}}\right). \tag{38}$$

Figure 8 presents the results obtained on the uncertain configuration given by

$$\begin{cases} U_0 = 1.0, \\ X \sim \mathcal{U}([-1,1]), \\ \sigma_s(X) = \sigma_a + \sigma_s + \nu_f \sigma_f(X), \\ \sigma_a = 0.6, \sigma_s = 0.1, \nu_f \sigma_f(X) = 0.1 + 0.21X, \\ \sigma_t = \sigma_a + \sigma_s + \sigma_f = 1.0. \end{cases} \tag{39}$$

Note that as X is uniformly distributed in $[-1,1]$, the Legendre basis is used for $(\phi_k(X))_{k\in\{0,\dots,P\}}$ (orthonormal with respect to the scalar product defined by the probability measure of X).

Configuration (39) is such that there is a probability of 1% for the medium to be multiplicative. Figure 8 compares, for several $(X_i)_{i\in\{1,\dots,N\}}$ (with $N = 30$ Gauss-Legendre points), the analytical results given by (36) to the one numerically estimated by averaging over several realisations of the stochastic process, i.e. $t \to \mathbb{E}[U_t(X_i)], i \in \{1,...,N\}$. On figure 8 (left), we can see that for some realisations of X, the number of particles grows fast or decays fast. The results in terms of first, i.e. $t \to \mathbb{E}[U_t(X)]$ (figure 8 left), and second, i.e. $t \to \mathbb{E}[U_t^2(X)]$ (figure 8 right), order moments of figure 8 are in excellent agreement for both moments, for every points $(X_i)_{i\in\{1,..,N\}}$.

Now, from expression (34), it is easy deducing the asymptotical variance of the estimated gPC coefficients: we asymptotically (i.e. for $N \gg 1$) have

$$\begin{aligned} \sigma^2_{k,\mathrm{sa}} &= \int \sigma^2_{\mathrm{sa}}(t,X)\phi_k(X)\,\mathrm{d}\mathcal{P}_X, \forall k \in \{0,...,P\}, \\ &= \int U_0^2(X) \left(e^{\dfrac{(v\sigma_s(X))^2 - (v\sigma_t(X))^2}{(v\sigma_t(X))} t} - e^{2(v\sigma_s(X)-v\sigma_t(X))t} \right) \phi_k(X)\,\mathrm{d}\mathcal{P}_X, \forall k \in \{0,...,P\}. \end{aligned} \tag{40}$$

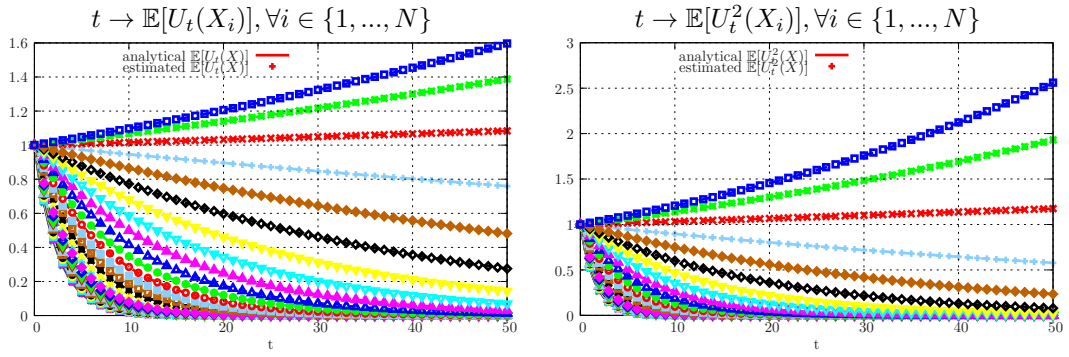

Figure 8: Comparisons of the time evolutions of $t \to \mathbb{E}[U_t(X_i)]$ (left) and $t \to \mathbb{E}[U_t^2(X_i)]$ (right) for $N = 30$ Gauss-Legendre points $(X_i)_{i \in \{1,...,N\}}$.

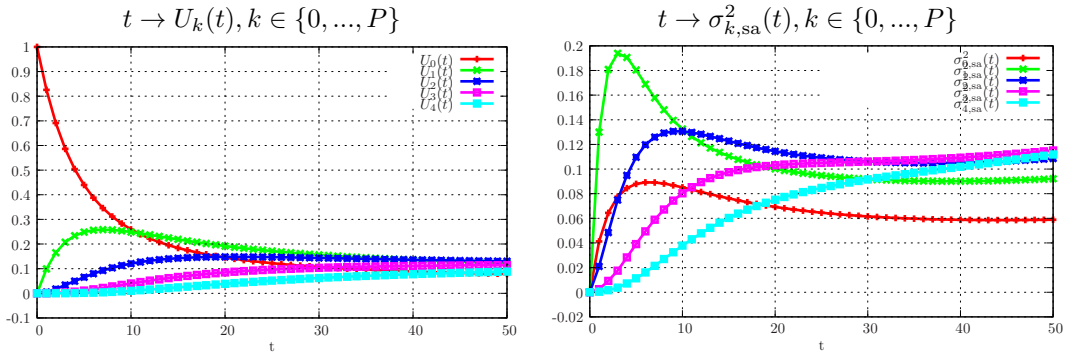

Figure 9: Time evolutions of $t \to U_k(t)$ (left) and $t \to \sigma^2_{k,\mathrm{sa}}(t)$ (right) in configuration (39) for $k \in \{0, ..., P = 4\}$.

This means that in this configuration, the error on the statistical quantities such as the mean, the variance, the gPC coefficients can be analytically characterised. The asymptotical variance (40) which measures the numerical error on the gPC coefficients in a non-intrusive applications will later on be compared to the asymptotical variances obtained with MC-gPC implemented with a semi-analog MC scheme.

Figure 9 presents the time evolutions of $t \to U_k(t), k \in \{0, ..., P = 4\}$ (left) and $t \to \sigma^2_{k,\mathrm{sa}}(t), k \in \{0, ..., P = 4\}$ (right) given by (40) in configuration (39). The projections on the gPC basis have been obtained by numerical integration (with $N = 30$ Gauss-Legendre points). On figure 9 (left), we can see that on average, the number of particles decreases with respect to time. The gPC coefficients are growing with respect to time attesting of an increasing uncertainty on the solution. On figure 9 (right), we can see that depending on the gPC coefficient, the numerical noise does not behave the same way: for early times, the error is first more important on $U_1(t)$ and $U_2(t)$. For later times, the errors on the $U_k(t)$ with $k > 2$ are more important.

Let us now perform the same analysis but for non-intrusive gPC applied on an MC code in which the non-analog MC scheme is implemented.

4.2.2. Non-intrusive non-analog MC schemes in the collisional regime

From (26), the variance of the error made $\forall X \in \mathrm{d}\mathcal{P}_X$ in a non-intrusive resolution is

$$\sigma^2_{\mathrm{na}}(t,X) = 0. \tag{41}$$

As a consequence, asymptotically with N_{MC}, according to the Central Limit Theorem, the error made on $U(t,X)$, $\forall X \in \mathrm{d}\mathcal{P}_X$ is given by

$$U(t,X) - U^{N_{MC}}(t,X) \sim \mathcal{G}\left(0, \frac{\sigma_{\mathrm{na}}(t,X)}{\sqrt{N_{MC}}}\right). \tag{42}$$

From expression (34), it is easy deducing the asymptotical error made when estimating the gPC coefficients: we asymptotically have, $\forall k \in \{0,...,P\}$

$$\sigma^2_{k,\mathrm{na}} = \int \frac{\sigma^2_{\mathrm{na}}(t,X)}{N_{MC}} \phi_k(X)\, \mathrm{d}\mathcal{P}_X = 0, \forall k \in \{0,...,P\}. \tag{43}$$

This means that in this configuration, the error on the statistical quantities such as the mean, the variance, the gPC coefficients can be analytically characterised. The asymptotical variance (43) which measures the numerical errors on the gPC coefficients in a non-intrusive applications will later on be compared to the asymptotical variances obtained with MC-gPC implemented with a semi-analog MC scheme.

4.3. MC-gPC for the semi- and non-analog MC schemes in the collisional regime

As explained before and detailed in [1, 6, 7], the MC-gPC implementation relies on few simple modifications of an existing MC code (see Appendix C for more details). The asymptotical variance of MC-gPC consequently strongly depends on the MC scheme implemented in the MC code. For this reason, in the two next sections, we study the asymptotical variances obtained from MC-gPC implemented in an MC code in which

- the semi-analog MC scheme is implemented, see section 4.3.1,
- the non-analog MC scheme is implemented, see section 4.3.2.

4.3.1. MC-gPC for the semi-analog MC scheme in the collisional regime

The starting point of the analysis is the expectation form of the uncertain transport equation (1) for the semi-analog MC scheme with the uncertain monokinetic, homogenous assumptions (i.e. $\sigma_\alpha(x,v,X) \equiv \sigma_\alpha(X), \forall \alpha \in \{s,t\}$ and $u(x,t,v,X) \equiv u(t,\omega,X)$). With these assumptions, the recursive equation (C.2) becomes

$$U_k(t) = \mathbb{E}\left[\mathbf{1}_{[t,\infty[}(\tau_X) U_0(X)\phi_k(X) + \mathbf{1}_{[0,t]}(\tau_X) U(t-\tau_X,X) \frac{\sigma_s(t-\tau_X,X)}{\sigma_t(t-\tau_X,X)} \phi_k(X)\right]. \tag{44}$$

We recall we have $X \sim \mathrm{d}\mathcal{P}_X$ and $\tau_X \sim \mathcal{E}(v\sigma_t(X))$. We suggest expanding the recursive part into an infinite sum over the number of interactions. Let us introduce a new random variable $S_i^X = \sum_{k=0}^{i} \tau_X^k$ where $\tau_X^k \sim \mathcal{E}(v\sigma_t(X))$ $\forall k \in \{1,...,i\}$ are independent identically distributed. Once again S_i^X follows a Gamma law of parameters $(v\sigma_t(X), i)$, denoted by $S_i^X \sim \Gamma(v\sigma_t(X), i)$.

Let us introduce $U_{t,l}$ the stochastic process induced by the possible histories of any MC particles. It is given by

$$U_{t,l} = \sum_{k=0}^{\infty} \mathbf{1}_{[0,t]}(S_k(X))\mathbf{1}_{[t,\infty[}(S_k(X) + \tau_X^{k+1}) \left(\frac{\sigma_s(X)}{\sigma_t(X)}\right)^k U_0(X)\phi_l(X).$$

The first moment is defined by $U_l(t) = \mathbb{E}[U_{t,l}]$, and by linearity its expression becomes

$$\begin{aligned} U_l(t) &= \mathbb{E}\left[U_{t,l}\right] = \mathbb{E}\left[\sum_{k=0}^{\infty} \mathbf{1}_{[0,t]}(S_k^X)\mathbf{1}_{[t,\infty[}(S_k^X + \tau_X^{k+1}) \left(\frac{\sigma_s(X)}{\sigma_t(X)}\right)^k U_0(X)\phi_l(X)\right], \\ &= \int U_0(X)\phi_l(X) \sum_{k=0}^{\infty} \mathbb{E}\left[\mathbf{1}_{[0,t]}(S_k^X)\mathbf{1}_{[t,\infty[}(S_k^X + \tau_X^{k+1})\right] \left(\frac{\sigma_s(X)}{\sigma_t(X)}\right)^k \mathrm{d}\mathcal{P}_X, \\ &= \int U_0(X)\phi_l(X) \sum_{k=0}^{\infty} \mathbb{P}\left(\tau_X^{k+1} > t - S_k^X | S_k^X < t\right) \left(\frac{\sigma_s(X)}{\sigma_t(X)}\right)^k. \end{aligned} \tag{45}$$

Replacing the probability of having k interactions by its expression (16) leads to

$$\begin{aligned} U_l(t) &= \int U_0(X)\phi_l(X) \sum_{k=0}^{\infty} e^{-v\sigma_t(X)t}(v\sigma_t(X))^k \frac{s^k}{k!} \left(\frac{v\sigma_s(X)}{v\sigma_t(X)}\right)^k \mathrm{d}\mathcal{P}_X, \\ &= \int U_0(X)\phi_l(X) e^{-v\sigma_t(X)t} \sum_{k=0}^{\infty} (v\sigma_s(X))^k \frac{s^k}{k!} \mathrm{d}\mathcal{P}_X, \\ &= \int U_0(X) e^{-v\sigma_a(X)t}\phi_l(X) \mathrm{d}\mathcal{P}_X. \end{aligned} \tag{46}$$

With the few previous computations, we formally verified the convergence of the semi-analog MC-gPC scheme for the gPC coefficients of the stochastic process $U_{t,l}$. Let us now study the moment of order 2 of the stochastic process $U_{t,l}$. It is defined as $\mathbb{E}\left[U_{t,l}^2\right]$ with

$$\begin{aligned} &U_{t,l}^2 = \\ &U_0^2(X)\phi_l^2(X) \sum_{i_1=0}^{\infty}\sum_{i_2=0}^{\infty} \mathbf{1}_{[0,t]}(S_{i_1}^X)\mathbf{1}_{[t,\infty[}(S_{i_1}^X + \tau_X^{i_1+1})\mathbf{1}_{[0,t]}(S_{i_2}^X))\mathbf{1}_{[t,\infty[}(S_{i_2}^X + \tau_X^{i_2+1}) \left(\frac{\sigma_s(X)}{\sigma_t(X)}\right)^{i_1+i_2}. \end{aligned}$$

In the previous expression, we expanded the exponant M into M summations over indices $(i_1, ..., i_M)$. Using the generalization to M terms of the fact that $\forall (k,m) \in \mathbb{N}^2$, we have

$$\mathbf{1}_{[0,t]}(S_k^X)\mathbf{1}_{[t,\infty[}(S_k^X + \tau_X^{k+1})\mathbf{1}_{[0,t]}(S_m^X)\mathbf{1}_{[t,\infty[}(S_m^X + \tau_X^{m+1}) = \delta_{k,m}\mathbf{1}_{[0,t]}(S_m^X)\mathbf{1}_{[t,\infty[}(S_m^X + \tau_X^{m+1}),$$

we simplify the above expression of $U_{t,l}^2(X)$ into

$$U_{t,l}^2 = U_0^2(X)\phi_l^2(X) \sum_{i=0}^{\infty} \mathbf{1}_{[0,t]}(S_i^X)\mathbf{1}_{[t,\infty[}(S_i^X + \tau_X^{i+1}) \left(\frac{\sigma_s(X)}{\sigma_t(X)}\right)^{2\times i}.$$

Taking the expectation of $U_{t,l}^2$ leads to

$$\begin{aligned}\mathbb{E}[U_{t,l}^2] &= \int U_0^2(X)\phi_l^2(X)\sum_{i=0}^{\infty}\mathbb{P}\left(\tau_X^{i+1} > t - S_i^X | S_i^X < t\right)\left(\frac{\sigma_s(X)}{\sigma_t(X}\right)^{2\times i}\mathrm{d}\mathcal{P}_X, \\ &= \int U_0^2(X)\phi_l^2(X)e^{-v\sigma_t(X)t}\sum_{i=0}^{\infty}(v\sigma_t(X))^i\frac{t^i}{i!}\left(\frac{\sigma_s(X)}{\sigma_t(X)}\right)^{2\times i}\mathrm{d}\mathcal{P}_X, \\ &= \int U_0^2(X)\phi_l^2(X)\exp\left(\frac{(v\sigma_s(X))^2-(v\sigma_t(X))^2}{(v\sigma_t(X))}t\right)\mathrm{d}\mathcal{P}_X.\end{aligned} \tag{47}$$

This leads to the asymptotic variance

$$\sigma_{l,\text{MC-sa}}^2(t) = \int U_0^2(X)\phi_l^2(X)\exp\left(\frac{(v\sigma_s(X))^2-(v\sigma_t(X))^2}{v\sigma_t(X)}t\right)\mathrm{d}\mathcal{P}_X - \left[\int U_0(X)e^{-v\sigma_a(X)t}\phi_l(X)\,\mathrm{d}\mathcal{P}_X\right]^2. \tag{48}$$

Figure 10 compares the results in terms of first and second order moments on the $P = 4$-truncated gPC coefficients obtained from

- the numerical integration of (48) (ref.),
- an estimation of (48) within an MC-gPC run,
- the time evolution of the variance estimated by relying on $N_{\text{seed}} = 1000$ runs with $N_{MC} = 100$ particles, each initialised with a different seed and by evaluating the variance of the random variable $(U_k(t) - \mathbb{E}[U_{k,t}])\sqrt{N_{MC}}, \forall k \in \{0, ..., P = 4\}$, i.e.

$$t \to \mathbb{V}\left[(U_k(t) - \mathbb{E}[U_{k,t}])\sqrt{N_{MC}}\right], \forall k \in \{0, ..., P = 4\}. \tag{49}$$

  According to the Central Limit Theorem (and due to the unbiasedness of the semi-analog estimator) we have $(U_k(t) - \mathbb{E}[U_{k,t}])\sqrt{N_{MC}} \sim \mathcal{G}(0, \sigma_{k,\text{MC-sa}}(t)), \forall k \in \{0, ..., P\}$.

The figure shows a good agreement which tends to verify both our implementation and analysis.

Now, expression (48) gives the asymptotic variance of the homogeneous process for the MC-gPC implementation within a semi-analog MC code. From the above expression, we can already tell that it differs from the one obtained in a non-intrusive context:

- first, this point has already been experimentally observed in [7]. We here have a proof in a particular configuration.
- Now, by comparing (48) for MC-gPC and (40) for non-intrusive gPC for $k = 0$, we can see that the error is the same on the mean $U_0(t)$ for the two resolution strategies (because we always have $\phi_0(X) = 1$ independently of $\mathrm{d}\mathcal{P}_X$ due to the orthonormality of the basis). In other words, if one compares the mean of an MC-gPC run and of a non-intrusive gPC study and observes a difference, this will only be explained by the numerical noise. The performance on the mean $U_0(t)$ are asymptotically the same.
- For higher order gPC coefficients ($k > 0$), there is a difference between (40) and (48) mainly explained by the exponant α of $\phi_k^\alpha(X)$: for (40), $\alpha = 1$ and for (48), $\alpha = 2$. In order to have a hint at what this exponant changes, let us consider a deterministic test-problem. In this regime, we have

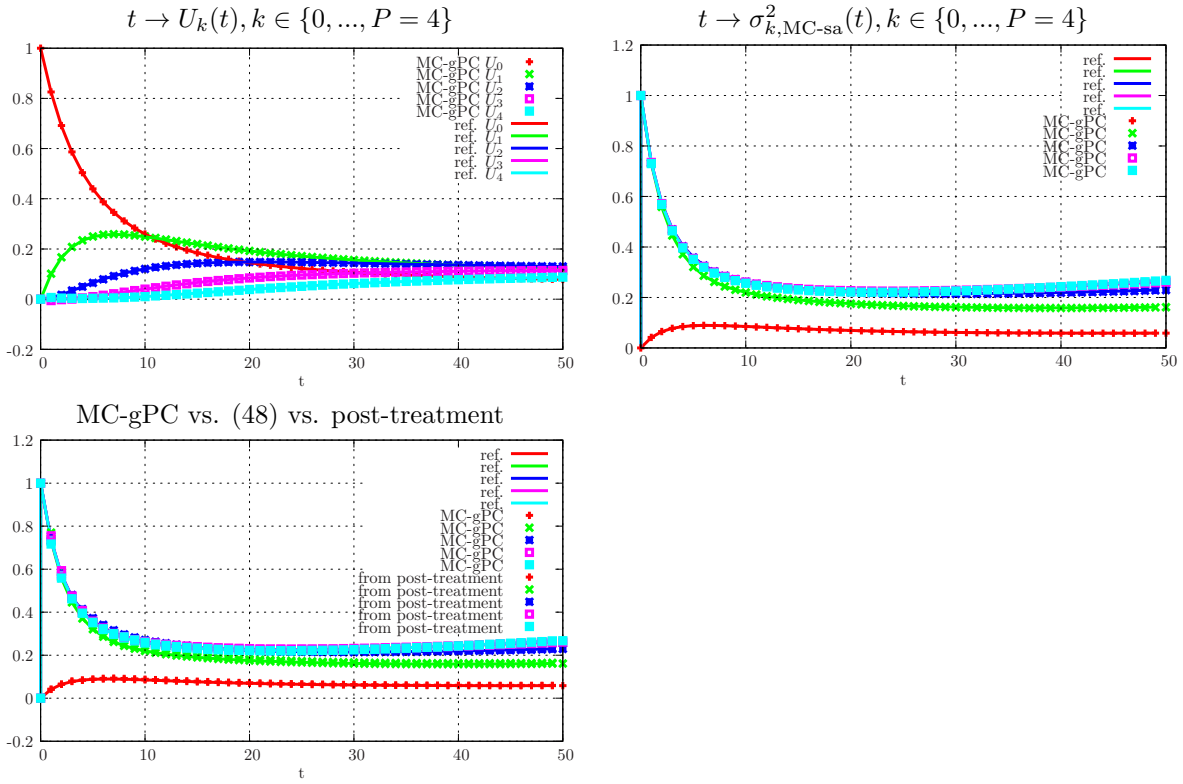

Figure 10: Top left: time evolution of the gPC coefficients $t \to U_k(t)\ \forall k \in \{0, ..., P = 4\}$ obtained with MC-gPC and analytically computed (ref.). Top right: time evolution of the variance multiplied by N_{MC} of the gPC coefficients $t \to \sigma^2_{k,\text{MC-sa}}(t)\ \forall k \in \{0, ..., P = 4\}$ obtained by instrumenting the semi-analog MC-gPC solver and analytically computed (ref.). Top right: time evolution of the variance multiplied by N_{MC} of the gPC coefficients $t \to \sigma^2_{k,\text{MC-sa}}(t)\ \forall k \in \{0, ..., P = 4\}$ obtained by instrumenting the semi-analog MC-gPC solver, an analytically computed reference (ref.) and an evalution by post-treatment of several runs of deterministic MC code (i.e. using (49)).

– from (40) for non-intrusive gPC

$$\begin{aligned}
\sigma^2_{k,\text{sa}}(t) &= \int U_0^2 \left(e^{\dfrac{(v\sigma_s)^2 - (v\sigma_t)^2}{(v\sigma_t)} t} - e^{2(v\sigma_s - v\sigma_t)t} \right) \phi_k(X)\, \mathrm{d}\mathcal{P}_X, \forall k \in \{0, ..., P\}, \\
&= U_0^2 \left(e^{\dfrac{(v\sigma_s)^2 - (v\sigma_t)^2}{(v\sigma_t)} t} - e^{2(v\sigma_s - v\sigma_t)t} \right) \int \phi_k(X)\, \mathrm{d}\mathcal{P}_X, \forall k \in \{0, ..., P\}, \\
&= \sigma^2_{\text{sa}}(t) \delta_{0,k}, \forall k \in \{0, ..., P\}.
\end{aligned}$$

From the above expression, we can see that in the deterministic regime, for $k > 0$, asymptotically, the error is zero as $\sigma^2_{k,\text{sa}}(t) = 0, \forall k \in \{1, ..., P\}$.

– From (48) for MC-gPC and $\forall k \in \{0, ..., P\}$

$$\begin{aligned}\sigma^2_{k,\text{MC-sa}}(t) &= \int U_0^2 \phi_l^2(X) \exp\left(\frac{(v\sigma_s)^2 - (v\sigma_t)^2}{(v\sigma_t)} t\right) \mathrm{d}\mathcal{P}_X - \left[\int U_0 e^{-v\sigma_a t} \phi_l(X)\, \mathrm{d}\mathcal{P}_X\right]^2, \\ &= U_0^2 \exp\left(\frac{(v\sigma_s)^2 - (v\sigma_t)^2}{(v\sigma_t)} t\right) \int \phi_l^2(X)\, \mathrm{d}\mathcal{P}_X - \left[U_0 e^{-v\sigma_a t} \int \phi_l(X)\, \mathrm{d}\mathcal{P}_X\right]^2, \\ &= U_0^2 \exp\left(\frac{(v\sigma_s)^2 - (v\sigma_t)^2}{(v\sigma_t)} t\right) - U_0 e^{-2v\sigma_a t} \delta_{k,0}.\end{aligned}$$

From the above expression, we can see that in the deterministic regime, for $k > 0$, asymptotically, the error is not zero as $\sigma^2_{k,\text{MC-sa}}(t) = U_0^2 \exp\left(\frac{(v\sigma_s)^2 - (v\sigma_t)^2}{(v\sigma_t)} t\right) \neq 0, \forall k \in \{1, ..., P\}$.

– From this relatively simple analysis, this means that there exists, for this MC scheme, regimes (at least the deterministic one) in which, asymptotically, MC-gPC can have lesser performances in terms of noise than non-intrusive gPC.

The last result is not alarming: first, MC-gPC has been experimentally computationally competitive in several configurations in which the semi-analog MC scheme was at the basis of the implementation, see [1, 6, 7]. One must not forget that the error in non-intrusive gPC and MC-gPC in not $\sigma_{k,\text{sa}}$ and $\sigma_{k,\text{MC-sa}}$ but rather $\frac{\sigma_{k,\text{sa}}}{\sqrt{N_{MC}}}$ and $\frac{\sigma_{k,\text{MC-sa}}}{\sqrt{N_{MC}}}$. The question now is: how many more MC-particles MC-gPC may need in order to have the same level of noise on the coefficients $(U_k(t))_{k\in\{0,...,P\}}$ as non-intrusive gPC? Having access to the analytical variances is handy in order to answer this question (indeed, otherwise, some false positive could be obtained only due to a coarse MC discretisation on one hand or the other): we suggest studying (40) and (48) more in details in the following paragraphs. Figure 11 compares (40) and (48) with respect to time in the configuration (39). Except for the mean (i.e. $k = 0$) for which the variances are exactly the same, non-intrusive gPC shows better performances in terms of noise. Now, depending on the time of interest, for $k > 0$, the numerical errors can be quite different. In figure 11, the worst case scenario happens for early times which, here, corresponds to having an almost deterministic solution: indeed, for early times, the solution $U(t, X) \sim U_0(X) = U_0$ in configuration (39). For early times, one must put more efforts in terms of number N_{MC} of particles for the semi-analog MC-gPC solver's accuracy to match the error the semi-analog non-intrusive one. Nonetheless, for later times, as the problem becomes uncertain, this gap in number of particles considerably drops and the performances of both resolution schemes become almost equivalent.

4.3.2. MC-gPC for the non-analog MC scheme in the collisional regime

The starting point of the analysis is the expectation form of the uncertain transport equation (1) for the non-analog MC scheme with the uncertain monokinetic, homogenous assumptions (i.e. $\sigma_\alpha(x, v, X) \equiv \sigma_\alpha(X), \forall \alpha \in \{s, t\}$ and $u(x, t, v, X) \equiv u(t, \omega, X)$). With these assumptions, the recursive equation (B.13) becomes

$$U_k(t) = \mathbb{E}\left[\mathbf{1}_{[t,\infty[}(\tau_X) U_0(X) e^{-v\sigma_a(X)t} \phi_k(X) + \mathbf{1}_{[0,t]}(\tau_X) U(t - \tau_X, X) e^{-v\sigma_a(X)(t-\tau_X)} \phi_k(X)\right]. \quad (50)$$

We recall we have $X \sim \mathrm{d}\mathcal{P}_X$ and $\tau_X \sim \mathcal{E}(v\sigma_s(X))$. We suggest expanding the recursive part into an infinite sum over the number of interactions. Let us introduce a new random variable $S_i^X = \sum_{k=0}^{i} \tau_X^k$ where $\tau_X^k \sim \mathcal{E}(v\sigma_s(X))\ \forall k \in \{1, ..., i\}$ are independent identically distributed.

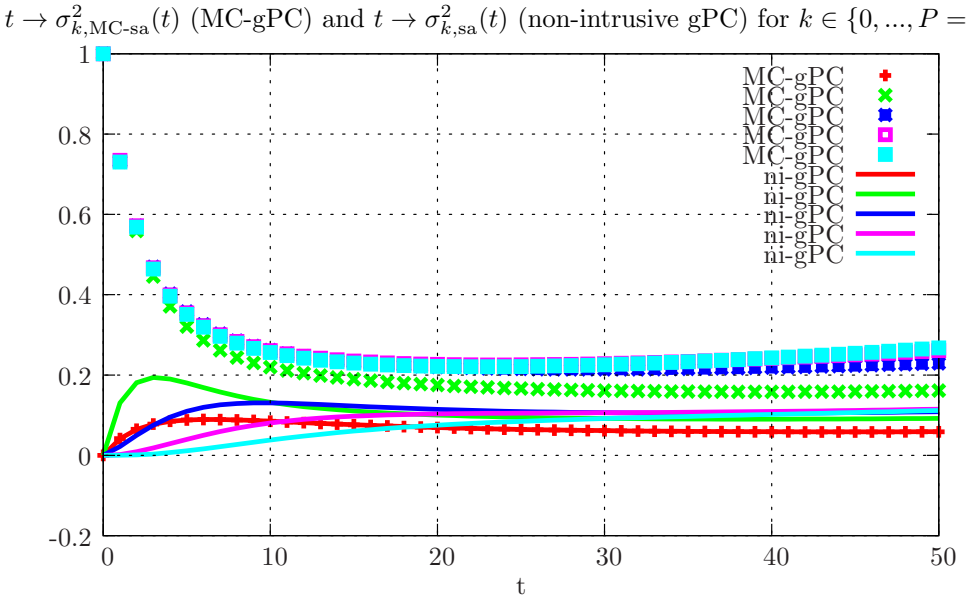

Figure 11: Comparison between $t \to \sigma^2_k(t)$ (non-intrusive gPC) and $t \to \sigma^2_{k,\text{MC-sa}}(t)$ (MC-gPC), for $k \in \{0, ..., P = 4\}$, both based on the semi-analog MC scheme.

Once again S_i^X follows a Gamma law of parameters $(v\sigma_s(X), i)$, denoted by $S_i^X \sim \Gamma(v\sigma_s(X), i)$. Let us introduce $U_{t,l}$ the stochastic process induced by the possible histories of any MC particles. It is given by

$$U_{t,l} = \sum_{k=0}^{\infty} \mathbf{1}_{[0,t]}(S_k(X))\mathbf{1}_{[t,\infty[}(S_k(X) + \tau_X^{k+1})e^{-v\sigma_a(X)\tau_X^{k+1}}U_0(X)\phi_l(X).$$

The first moment is defined by $U_l(t) = \mathbb{E}[U_{t,l}]$, and by linearity its expression becomes

$$\begin{aligned} U_l(t) &= \mathbb{E}\left[U_{t,l}\right] = \mathbb{E}\left[\sum_{k=0}^{\infty} \mathbf{1}_{[0,t]}(S_k^X)\mathbf{1}_{[t,\infty[}(S_k^X + \tau_X^{k+1})e^{-v\sigma_a(X)\tau_X^{k+1}}U_0(X)\phi_l(X)\right], \\ &= \int U_0(X)\phi_l(X) \sum_{k=0}^{\infty} \mathbb{E}\left[\mathbf{1}_{[0,t]}(S_k^X)\mathbf{1}_{[t,\infty[}(S_k^X + \tau_X^{k+1})\right] e^{-v\sigma_a(X)\tau_X^{k+1}} \,\mathrm{d}\mathcal{P}_X, \\ &= \int U_0(X)\phi_l(X)e^{-v\sigma_a(X)t} \sum_{k=0}^{\infty} \mathbb{P}\left(\tau_X^{k+1} > t - S_k^X | S_k^X < t\right). \\ &= \int U_0(X)e^{-v\sigma_a(X)t}\phi_l(X) \,\mathrm{d}\mathcal{P}_X. \end{aligned} \tag{51}$$

With the few previous computations, we formally verified the convergence of the non-analog MC-gPC scheme for the gPC coefficients of the stochastic process U_t. Let us now study the moment of

order 2 of the stochastic process $U_{t,l}$. It is defined as $\mathbb{E}\left[U_{t,l}^2\right]$ with

$$U_{t,l}^2 = U_0^2(X)\phi_l^2(X)\sum_{i_1=0}^{\infty}\sum_{i_2=0}^{\infty}\mathbf{1}_{[0,t]}(S_{i_1}^X)\mathbf{1}_{[t,\infty[}(S_{i_1}^X+\tau_X^{i_1+1})\mathbf{1}_{[0,t]}(S_{i_2}^X))\mathbf{1}_{[t,\infty[}(S_{i_2}^X+\tau_X^{i_2+1})e^{-v\sigma_a(X)(t-\tau_X^{i_1+1})}e^{-v\sigma_a(X)(t-\tau_X^{i_2+1})}.$$

In the previous expression, we expanded the exponant M into M summations over indices $(i_1,...,i_M)$. Using the generalization to M terms of the fact that $\forall(k,m)\in\mathbb{N}^2$, we have

$$\mathbf{1}_{[0,t]}(S_k^X)\mathbf{1}_{[t,\infty[}(S_k^X+\tau_X^{k+1})\mathbf{1}_{[0,t]}(S_m^X)\mathbf{1}_{[t,\infty[}(S_m^X+\tau_X^{m+1}) = \delta_{k,m}\mathbf{1}_{[0,t]}(S_m^X)\mathbf{1}_{[t,\infty[}(S_m^X+\tau_X^{m+1}),$$

we simplify the above expression of $U_{l,t}^2(X)$ into

$$U_{t,l}^2 = U_0^2(X)\phi_l^2(X)\sum_{i=0}^{\infty}\mathbf{1}_{[0,t]}(S_i^X)\mathbf{1}_{[t,\infty[}(S_i^X+\tau_X^{i+1})e^{-v\sigma_a(X)2(t-\tau_X^{i+1})}.$$

Taking the expectation of $U_{t,l}^2$ leads to

$$\begin{aligned}\mathbb{E}[U_{t,l}^2] &= \int U_0^2(X)\phi_l^2(X)\sum_{i=0}^{\infty}\mathbb{P}\left(\tau_X^{i+1}>t-S_i^X|S_i^X<t\right)e^{-v\sigma_a(X)2(t-\tau_X^{i+1})}\,\mathrm{d}\mathcal{P}_X,\\ &= \int U_0^2(X)\phi_l^2(X)e^{-2v\sigma_t(X)t}\,\mathrm{d}\mathcal{P}_X.\end{aligned} \tag{52}$$

For the variance, we finally get

$$\sigma_{l,\text{MC-na}}^2(t) = \int U_0^2(X)\phi_l^2(X)e^{-2v\sigma_a(X)t}\,\mathrm{d}\mathcal{P}_X - \left[\int U_0(X)e^{-v\sigma_a(X)t}\phi_l(X)\,\mathrm{d}\mathcal{P}_X\right]^2. \tag{53}$$

Figure 12 compares the results in terms of first and second order moments on the $P=4$-truncated gPC coefficients obtained from

- the numerical integration of (53) (ref.),
- an estimation of (53) within an MC-gPC run,
- the time evolution of the variance estimated by relying on $N_{\text{seed}}=1000$ runs with $N_{MC}=100$ particles, each initialised with a different seed and by evaluating the variance of the random variable $(U_k(t)-\mathbb{E}[U_{k,t}])\sqrt{N_{MC}},\forall k\in\{0,...,P=4\}$, i.e.

$$t\to\mathbb{V}\left[(U_k(t)-\mathbb{E}[U_{k,t}])\sqrt{N_{MC}}\right],\forall k\in\{0,...,P=4\}. \tag{54}$$

  According to the Central Limit Theorem (and due to the unbiasedness of the semi-analog estimator) we have $(U_k(t)-\mathbb{E}[U_{k,t}])\sqrt{N_{MC}}\sim\mathcal{G}(0,\sigma_{k,\text{MC-na}}(t)),\forall k\in\{0,...,P\}$.

The figure shows a good agreement which tends to verify both our implementation and analysis (V&V [41]) of MC-gPC combined to the non-analog MC scheme together with the unbiasedness of our estimators.

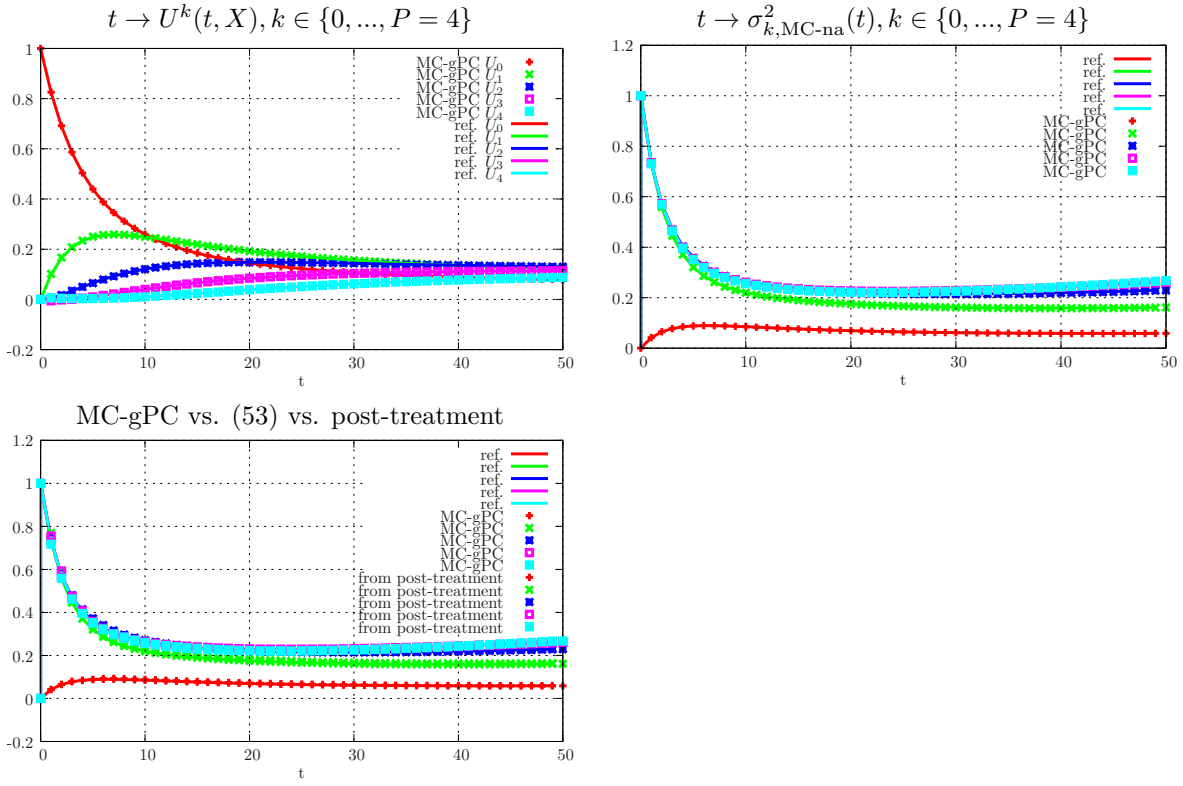

Figure 12: Top left: time evolution of the gPC coefficients $t \to U_k(t)\ \forall k \in \{0,...,P=4\}$ obtained with MC-gPC and analytically computed (ref.) for the non-analog MC scheme. Top right: time evolution of the variance multiplied by N_{MC} of the gPC coefficients $t \to \sigma^2_{k,\text{MC-na}}(t)\ \forall k \in \{0,...,P=4\}$ obtained by instrumenting the non-analog MC-gPC solver and analytically computed (ref.). Top right: time evolution of the variance multiplied by N_{MC} of the gPC coefficients $t \to \sigma^2_{k,\text{MC-na}}(t)\ \forall k \in \{0,...,P=4\}$ obtained by instrumenting the non-analog MC-gPC solver, an analytically computed reference (ref.) and an evalution by post-treatment of several runs of deterministic MC code (i.e. using (54)).

Now, we can compare the asymptotical variances obtained with non-intrusive gPC and MC-gPC, both based on a non-analog MC resolution. Once again, except for the first gPC coefficient u_0, the asymptotical variances are more important with MC-gPC than with non-intrusive gPC. The conclusions are actually the same as for the semi-analog MC scheme of the previous section. *Note that in the collisional regime, with the non-analog MC scheme, the loss between non-intrusive gPC and MC-gPC is quite important in terms of numerical error (as the variance is zero for non-intrusive gPC with the non-analog MC scheme).*

We finally compare, on figure 13, the asymptotical variances of a semi-analog MC-gPC implementation and of a non-analog MC-gPC implementation. For every gPC coefficients and for every times, in the collisional regime, the error with the semi-analog MC-gPC scheme is slightly higher than for the non-analog MC-gPC one. The improvement ensured by the non-analog MC scheme in the collisional regime is not significative for MC-gPC (whereas it is for non-intrusive gPC).

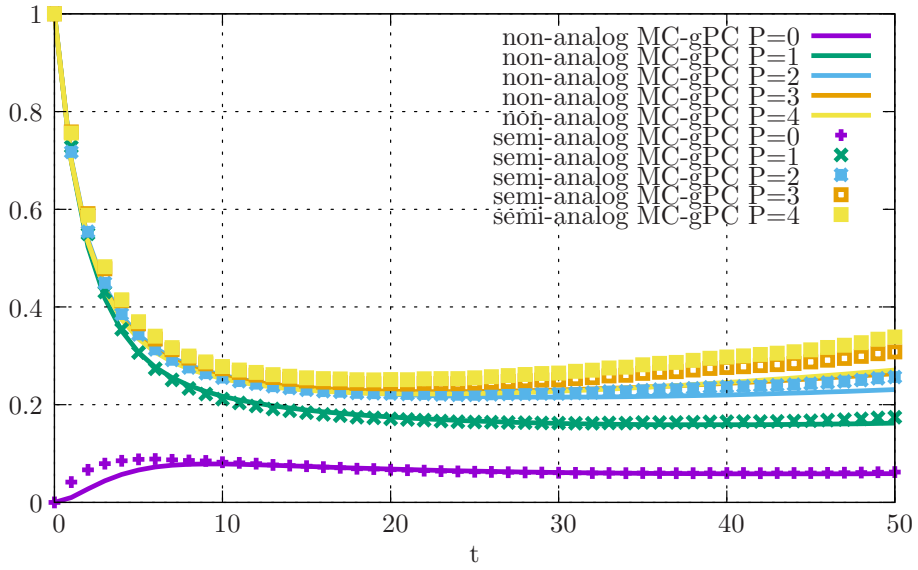

Figure 13: Time evolutions of $t \to \sigma^2_{k,\mathrm{sa}}(x,t)$ and $t \to \sigma^2_{k,\mathrm{na}}(x,t)$for $k \in \{0,...,P=4\}$ (i.e. for non-analog MC-gPC and semi-analog MC-gPC).

5. Discussion on how to use the previous results and conclusion

In this paper, we studied the numerical noise induced by the Monte-Carlo resolution of (intrusive and non-intrusive) gPC based reduced model. In particular, we deepened the study of MC-gPC applied to the uncertain linear Boltzmann equation. We theoretically and numerically compare the variances (which are estimators of the error for the unbiased MC schemes) of combinations of MC schemes/uncertainty propagation methods (the semi- and non-analog ones and non-intrusive gPC and MC-gPC). In this concluding section, we give examples of how the material of the previous sections can be used in practice. In particular, we think the analysis can help verify MC codes (section 5.1), help decide which solver is more appropriate to one's problem of interest (section 5.2), help predict the behaviour of the numerical noise on statistical quantities of interest (section 5.3) and help identify the weaknesses of MC-gPC in order to imagine new ways to improve it (section 5.4).

5.1. Help verify an MC code implementation (Verification & Validation [41])

The first use for the previous material which comes in mind concerns Verification & Validation V&V [41] and especially verification. For example,

- the high order moments of the semi-analog (section 3.2.1) and of the non-analog (section 3.2.2) MC schemes and their asymptotical variances in the collisional regime can be used to verify the implementation of some deterministic MC code.
- The asymptotical variances obtained in the different sections (in the deterministic or uncertain case) allow verifying the unbiasedness of the estimator (in the free-flight regime and the collisional one, see sections 3.1–3.2.1–3.2.2–4.3.1–4.3.2).

– The asymptotical variances of the gPC coefficients for non-intrusive and MC-gPC allow verifying the implementations of non-intrusive gPC but, above all, MC-gPC, independently of the MC scheme (semi-analog or non-analog) already implemented in the deterministic MC code from which MC-gPC is based (sections 4.3.1–4.3.2).

With these examples, the results of the different sections are considered independently. By comparing them, we can go further and make advised choices in order to obtain better performances for our resolution schemes.

5.2. Help in decision making

From the previous differences, depending on the regime of interest, we can discuss our choices:

– suppose one has mainly to consider configurations in the deterministic collisional regime, then the non-analog MC scheme is more efficient than the semi-analog one.

– Suppose one is willing to implement MC-gPC within an MC code in which the semi-analog MC scheme is implemented: then it is almost pointless to implement the non-analog one first hand as with MC-gPC, the semi-analog and the non-analog MC schemes have almost the same performances.

– If one wants to stick with non-intrusive gPC, an MC code with the non-analog MC scheme is more efficient (same performances as the semi-analog one in the free flight regime and zero variance on the gPC coefficients in the collisional one, see sections 3.1–4.2).

The above list is non-exhaustive and we can also use the above material for more practical considerations, see the two next sections.

5.3. Help predict the behaviour of the numerical noise/error on some statistical quantities

The previous analysis can also help deducing confidence bounds on the different statistical quantities of interest. The most obvious example remains the one of the mean for which we have for MC-gPC

$$\mathbb{E}[u^{N_{MC}}(x,t,v,X)] = u_0^{N_{MC}}(x,t,v) = u_0(x,t,v) + \frac{\sigma_0(x,t,v)}{\sqrt{N_{MC}}}\mathcal{G}_0.$$

It gives an idea of how the approximation of the mean is improved with the N_{MC} the number of MC particles in the simulations. For the mean, it corresponds to a direct application of the material of the previous sections (see section 4.3 for MC-gPC).

On another hand, a less direct application corresponds to the study of the numerical noise on other statistical quantities of interest: let us take the example of the physical variance. It can be obtained from the gPC coefficients as (see [50] for example)

$$\mathbb{V}[u^{N_{MC}}(x,t,v,X)] \quad = \sum_{k=1}^{P} \left(u_k^{N_{MC}}(x,t,v)\right)^2.$$

Using the material of the previous section, we can relate the physical variance obtained from an MC approximation to the analytical one as we have:

$$\begin{aligned}
\mathbb{V}[u^{N_{MC}}(x,t,v,X)] &= \sum_{k=1}^{P}\left(u_k^{N_{MC}}(x,t,v)\right)^2, \\
&= \sum_{k=1}^{P}\left(u_k(x,t,v)+\frac{\sigma_k(x,t,v)}{\sqrt{N_{MC}}}\mathcal{G}_k\right)^2, \\
&= \sum_{k=1}^{P}\left(u_k(x,t,v)\right)^2+\sum_{k=1}^{P}u_k(x,t,v)\frac{\sigma_k(x,t,v)}{\sqrt{N_{MC}}}\mathcal{G}_k+\sum_{k=1}^{P}\left(\frac{\sigma_k(x,t,v)}{\sqrt{N_{MC}}}\mathcal{G}_k\right)^2, \\
&= \mathbb{V}[u(x,t,v)]+\sum_{k=1}^{P}u_k(x,t,v)\frac{\sigma_k(x,t,v)}{\sqrt{N_{MC}}}\mathcal{G}_k+\sum_{k=1}^{P}\left(\frac{\sigma_k(x,t,v)}{\sqrt{N_{MC}}}\mathcal{G}_k\right)^2.
\end{aligned}$$

From the above expression, we can deduce that by averaging over several runs (i.e. several seeds), we asymptotically have

$$\mathbb{E}\left[\mathbb{V}[u^{N_{MC}}(x,t,v,X)]\right] = \mathbb{E}\left[\mathbb{V}[u(x,t,v)]\right]+\sum_{k=1}^{P}\frac{\sigma_k^2(x,t,v)}{N_{MC}}.$$

The above expression is interesting in the sense that estimating the variances $(\sigma_k^2)_{k\in\{0,\dots,P\}}$ together with the physical variance $\mathbb{V}[u^{N_{MC}}(x,t,v,X)]$ can lead to the estimation of an upper bound of the true physical variance $\mathbb{V}[u(x,t,v,X)]$ (which is often desired in industrial applications) of the quantity of interest. Of course, the previous analysis can be carried out on other statistical quantities (Sobol indices for sensitivity analysis etc.) which can be deduced from the gPC coefficients, see [43, 56].

5.4. Help understand the weaknesses and improvements for MC-gPC

Finally, with the previous analysis, we also identified explicitly the term which is problematic for MC-gPC: in section 4.3, we saw that the estimator of the second order moment uses ϕ_k^α with $\alpha = 2$ for MC-gPC (where non-intrusive gPC uses ϕ_k^α with $\alpha = 1$). This exponant $\alpha = 2$ induces a loss in terms of variance, especially in the deterministic case (or more generally when the gPC coefficients are small), see sections 4.1.2–4.3. This is probably the weakest point of MC-gPC. It has been precisely identified thanks to the previous analysis. From what we just learnt, we can now imagine ways to avoid this excess of variance and improve MC-gPC: for example, there are several ways to solve the reduced model (C.1) at the basis of MC-gPC. Until now, the MC resolution of system (C.1) was based on an MC scheme allowing having minimal and simple modifications of an existing MC solver, see [1] and Appendix C. But these minimal and simple modifications are not the only ones ensuring solving the gPC based reduced model (C.1). New numerical strategies could be designed in order to avoid having a too important noise in the deterministic regime. For example, system (C.1) has almost the same structure as a multi-group system [15, 13]. We could consequently use already existing strategies in order to reduce the noise of the MC resolution of the reduced model (C.1) using multi-group MC schemes (for which $(\phi_k)_{k\in\{0,\dots,P\}}$ is not anymore explicitly involved in the estimator of the first or second order moments of the stochastic process allowing to approximate the solution of our PDE set). This strategy would certainly lead to less simple modifications of an existing MC solver but also probably to important improvements. This will be the purpose of further publications.

References

[1] G. Poëtte, A gPC-intrusive Monte Carlo scheme for the resolution of the uncertain linear Boltzmann equation, Journal of Computational Physics 385 (2019) 135 – 162. doi:https://doi.org/10.1016/j.jcp.2019.01.052.
URL http://www.sciencedirect.com/science/article/pii/S002199911930110X

[2] G. Poëtte, Spectral convergence of the generalized polynomial chaos reduced model obtained from the uncertain linear boltzmann equation, Mathematics and Computers in Simulation 177 (2020) 24–45. doi:https://doi.org/10.1016/j.matcom.2020.04.009.
URL https://www.sciencedirect.com/science/article/pii/S037847542030121X

[3] J. A. Carrillo, M. Zanella, Monte Carlo gPC methods for diffusive kinetic flocking models with uncertainties Preprint (2019).

[4] L. Pareschi, An introduction to uncertainty quantification for kinetic equations and related problems (2020). arXiv:2004.05072.

[5] L. Pareschi, M. Zanella, Monte Carlo stochastic Galerkin methods for the Boltzmann equation with uncertainties: space-homogeneous case (03 2020). doi:10.13140/RG.2.2.28177.17760.

[6] G. Poëtte, Efficient uncertainty propagation for photonics: Combining implicit semi-analog monte carlo (ismc) and monte carlo generalised polynomial chaos (mc-gpc), Journal of Computational Physics (2021) 110807doi:https://doi.org/10.1016/j.jcp.2021.110807.
URL https://www.sciencedirect.com/science/article/pii/S0021999121007026

[7] G. Poëtte, E. Brun, Efficient uncertain k eff computations with the Monte Carlo resolution of generalised Polynomial Chaos Based reduced models, working paper or preprint (Nov. 2020).
URL https://hal.archives-ouvertes.fr/hal-02996843

[8] R. A. Todor, C. Schwab, Karhunen-Loève approximation of random fields by generalized fast multipole methods, J. Comp. Phys. 217 (1) (2006) 100–122.

[9] M. Meyer, H. Matthies, Efficient model reduction in non-linear dynamics using the Karhunen-Loève expansion and dual-weighted-residual methods, Comp. Meth. Appl. Mech. Eng. Informatikbericht 2003-08, TU Braunschweig, Germany (2004).

[10] J. Mercer, Functions of Positive and Negative Type and their Connection with the Theory of Integral Equations, Philos. Trans. Roy. Soc. 209 (1909).

[11] R. Lebrun, A. Dutfoy, A Generalization of the Nataf Transformation to Distributions with Elliptical Copula, Prob. Eng. Mech. 24,2 (2009) 172–178.

[12] R. Lebrun, A. Dutfoy, An Innovating Analysis of the Nataf Transformation from the Copula viewpoint, Prob. Eng. Mech. 24,3 (2009) 312–320.

[13] J. Spanier, E. M. Gelbard, Monte Carlo Principles and Neutron Transport Problems, Addison-Wesley, 1969.

[14] E. E. Lewis and W. F. Miller Jr., Computational Methods of Neutron Transport, John Wiley and Son New York, 1984.

[15] G. Bell, S. Gladstone, Nuclear Reactor Theory, Van Nostrand Reinhold Company, 1970.
URL https://books.google.fr/books?id=RNQmAQAAMAAJ

[16] F. Golse, G. Allaire, Transport et Diffusion, 2015, polycopié de cours.

[17] B. Iooss, P. Lemaître, A Review on Global Sensitivity Analysis Methods, Dellino, Gabriella and Meloni, Carlo, Springer US, Boston, MA, 2015, pp. 101–122. doi:10.1007/978-1-4899-7547-8_5.
URL http://dx.doi.org/10.1007/978-1-4899-7547-8_5

[18] E. Brun, S. Chauveau, F. Malvagi, Patmos: A prototype Monte Carlo transport code to test high performance architectures, In Proceedings of International Conference on Mathematics & Computational Methods Applied to Nuclear Science & Engineering, Jeju, Korea, 2017.

[19] E. Brun, F. Damian, C. Diop, E. Dumonteil, F. Hugot, C. Jouanne, Y. Lee, F. Malvagi, A. Mazzolo, O. Petit, J. Trama, T. Visonneau, A. Zoia, Tripoli-4®, cea, edf and areva reference monte carlo code, Annals of Nuclear Energy 82 (2015) 151 – 160, joint International Conference on Supercomputing in Nuclear Applications and Monte Carlo 2013, SNA + MC 2013. Pluri- and Trans-disciplinarity, Towards New Modeling and Numerical Simulation Paradigms. doi:https://doi.org/10.1016/j.anucene.2014.07.053.
URL http://www.sciencedirect.com/science/article/pii/S0306454914003843

[20] T. Goorley, MCNP6.1.1-Beta Release Notes LA-UR-14-24680 (2014).

[21] J. A. Fleck, J. D. Cummings, An implicit monte-carlo scheme for calculating time and frequency dependent nonlinear radiation transport, Journal of Computational Physics (1971).

[22] R. P. Smedley-Stevenson, R. G. McClarren, Asymptotic diffusion limit of cell temperature discretisation schemes for thermal radiation transport, Journal of Computational Physics 286 (2015) 214 – 235. doi:https://doi.org/10.1016/j.jcp.2013.10.038.
URL http://www.sciencedirect.com/science/article/pii/S0021999113007146

[23] J.-F. Clouet, G. Samba, Asymptotic diffusion limit of the symbolic monte carlo method for the transport equation, Journal of Computational Physics 195 (1) (2004) 293 – 319. doi:https://doi.org/10.1016/j.jcp.2003.10.008.
URL http://www.sciencedirect.com/science/article/pii/S0021999103005333

[24] G. Poëtte, X. Valentin, A new implicit monte-carlo scheme for photonics (without teleportation error and without tilts), Journal of Computational Physics 412 (2020) 109405. doi:https://doi.org/10.1016/j.jcp.2020.109405.
URL http://www.sciencedirect.com/science/article/pii/S0021999120301790

[25] E. Steinberg, S. I. Heizler, Multi-frequency implicit semi-analog monte-carlo (ismc) radiative transfer solver in two-dimensions (without teleportation) (2021). arXiv:2108.02612.

[26] B. Perthame, Transport Equations in Biology, Birkhauser Verlag, Basel Boston Berlin, 2000.

[27] L. Pareschi, P. Vellucci, M. Zanella, Kinetic models of collective decision-making in the presence of equality bias, Physica A: Statistical Mechanics and its Applications 467 (2017) 201 – 217. doi:https://doi.org/10.1016/j.physa.2016.10.003.
URL http://www.sciencedirect.com/science/article/pii/S0378437116306902

[28] B. M. Althouse, E. A. Wenger, J. C. Miller, S. V. Scarpino, A. Allard, L. Hébert-Dufresne, H. Hu, Stochasticity and heterogeneity in the transmission dynamics of sars-cov-2, 2020.

[29] B. Lapeyre, E. Pardoux, R. Sentis, Méthodes de Monte Carlo pour les équations de transport et de diffusion, no. 29 in Mathématiques & Applications, Springer-Verlag, 1998.

[30] M. Coste-Delclaux, C. DIOP, A. NICOLAS, B. BONIN, Neutronique, E-den, Une monographie de la Direction de l'énergie nucléaire, CEA Saclay; Groupe Moniteur, 2013.
URL https://hal-cea.archives-ouvertes.fr/cea-01152822

[31] D. Dureau, G. Poëtte, Hybrid Parallel Programming Models for AMR Neutron Monte Carlo Transport, in: Joint International Conference on Supercomputing in Nuclear Applications + Monte Carlo, no. 04202 in Parallelism and HPC, Monte Carlo, 2013.

[32] Martin, William R., et al., Monte Carlo photon transport on shared memory and distributed memory parallel processors, International Journal of High Performance Computing Applications 1.3 (1987) 57–74.

[33] Parallel performance study of monte carlo photon transport code on shared-, distributed-, and distributed-shared-memory architectures, Parallel and Distributed Processing Symposium, 2000.

[34] G. Poëtte, Contribution to the mathematical and numerical analysis of uncertain systems of conservation laws and of the linear and nonlinear boltzmann equation, Habilitation à diriger des recherches, Université de Bordeaux 1 (Sep. 2019).
URL https://hal.archives-ouvertes.fr/tel-02288678

[35] C. Ahrens, E. Larsen, A semi-analog monte carlo method for grey radiative transfer problems, in: Proceedings of the ANS Topical Meeting: International Conference on Mathematical Methods to Nuclear Applications, 2001.

[36] J. A. F. Jr., The calculation of nonlinear radiation transport by a monte carlo method, Tech. rep., Lawrence Radiation Laboratory, University of California (1961).

[37] M. S. McKinley, E. D. B. III, A. Szoke, Comparison of implicit and symbolic implicit monte carlo line transport with frequency weight vector extension, Journal of Computational Physics (2003).

[38] A. G. Irvine, I. D. Boyd, N. A. Gentile, Reducing the spatial discretization error of thermal emission in implicit monte carlo simulations, Journal of Computational and Theoretical Transport 45 (1-2) (2016) 99–122. arXiv:https://doi.org/10.1080/23324309.2015.1060245, doi:10.1080/23324309.2015.1060245.
URL https://doi.org/10.1080/23324309.2015.1060245

[39] G. Poëtte, X. Valentin, A. Bernede, Canceling teleportation error in legacy imc code for photonics (without tilts, with simple minimal modifications), Journal of Computational and Theoretical Transport 49 (4) (2020) 162–194. arXiv:https://doi.org/10.1080/23324309.2020.1785893, doi:10.1080/23324309.2020.1785893.
URL https://doi.org/10.1080/23324309.2020.1785893

[40] E. Steinberg, S. I. Heizler, Discrete implicit monte-carlo (dimc) scheme for simulating radiative transfer problems (2021). arXiv:2108.13453.

[41] A. S. o. M. E. ASME V&V 20-2009, Standard for Verification and Validation in Computational Fluid Dynamics and Heat Transfer, ASME (2009).

[42] G. Blatman, Adaptive sparse polynomial chaos expansions for uncertainty propagation and sensitivity analysis, Thèse de doctorat, Université Blaise Pascal - Clermont II (2009).

[43] G. Blatman, B. Sudret, Sparse Polynomial Chaos Expansions and Adaptive Stochastic Finite Elements using a Regression Approach, C. R. Méc. 336 (2008) 518–523. doi:10.1016/j.crme.2008.02.013.

[44] T. Crestaux, Polynômes de Chaos pour la Propagation et la Quantification d'Incertitudes, Tech. rep., CEA (2006).

[45] N. Wiener, The Homogeneous Chaos, Amer. J. Math. 60 (1938) 897–936.

[46] R. Cameron, W. Martin, The Orthogonal Development of Non-Linear Functionals in Series of Fourier-Hermite Functionals, Annals of Math. 48 (1947) 385–392.

[47] Ernst, Oliver G., Mugler, Antje, Starkloff, Hans-Jörg, Ullmann, Elisabeth, On the convergence of generalized polynomial chaos expansions, ESAIM: M2AN 46 (2) (2012) 317–339. doi:10.1051/m2an/2011045.
URL `https://doi.org/10.1051/m2an/2011045`

[48] F. Simon, P. Guillen, P. Sagaut, D. Lucor, A gPC based approach to uncertain transonic aerodynamics, CMAME 199 (2010) 1091–1099.

[49] D. Lucor, J. Meyers, P. Sagaut, Sensitivity Analysis of LES to Subgrid-Scale-Model Parametric Uncertainty using Polynomial Chaos, J. Fluid Mech. 585 (2007) 255–279.

[50] J.-M. Martinez, J. Cahen, A. Millard, D. Lucor, F. Huvelin, J. Ko, N. Poussineau, Modélisation des Incertitudes par Polynômes de Chaos – Étude d'un Écoulement en Milieux Poreux, Tech. Rep. Rapport DM2S/DIR/RT/06-006/A, CEA-CEMRACS (2006).

[51] B. Sudret, Uncertainty Propagation and Sensitivity Analysis in Mechanical Models, Contribution to Structural Reliability and Stochastic Spectral Methods, Habilitation à Diriger des Recherches, Université Blaise Pascal - Clermont II (2007).

[52] M. Berveiller, B. Sudret, M. Lemaire, Stochastic Finite Element: a Non Intrusive Approach by Regression, Rev. Eur. Méc. Num. 15 (1-2-3) (2006) 81–92.

[53] B. Méchitoua, On the fictitious aspect of the critical state, JAERI-Conf 019, jP0450146 (2003).

[54] B. Mechitoua, Tokaimura criticality accident: Point model stochastic neutronic interpretation, ANS Annual Meeting (2001).

[55] D. Verwaerde, Une approche non déterministe de la neutronique - modélisation, Tech. rep., CEA (1993).

[56] G. Blatman, B. Sudret, Efficient computation of global sensitivity indices using sparse polynomial chaos expansions, Rel. Eng. Syst. Saf. 95 (2010) 1216–1229.

Appendix A. A simple analytical uncertain solution

In this section we build an analytical solution in a simple uncertain configuration. It is used as a reference solution for the convergence studies of section 2 and figure 1. The configuration is monokinetic (i.e. $v = 1$) and homogeneous (i.e. $u(x,t,\mathbf{v},X) = u(t,\omega,X)$). We assume the uncertainty, one-dimensional here for the sake of simplicity, affects the scattering cross-sections $\sigma_s = \overline{\sigma}_s + \hat{\sigma}_s X$, where $X \sim \mathcal{U}[-1,1]$ and $\hat{\sigma}_s$ is closely related to the variance of the uncertain scattering cross-section. Let us introduce $U(t,X) = \iint u(x,t,\omega,X)\,\mathrm{d}x\,\mathrm{d}\omega$. In the previously described configuration, the uncertain linear Boltzmann equation resumes to the following stochastic ordinary differential equation

$$\begin{cases} \partial_t U(t,X) + v\sigma_t U(t,X) = v\sigma_s(X)U(t,X), \\ U(0) = U_0, \end{cases} \tag{A.1}$$

satisfied by U. Introduce $\sigma_a = \sigma_t - \sigma_s$, then the solution is given by

$$U(t,X) = U_0 e^{-v\sigma_a(X)t} = U_0 e^{-v(\sigma_t - \overline{\sigma}_s - \hat{\sigma}_s X)t} = U_0 e^{-v(\overline{\sigma}_a - \hat{\sigma}_s X)t}. \tag{A.2}$$

The quantity $U(t,X)$ is a random variable indexed by time t, i.e. it is a stochastic process. In this case, mean and variance of the stochastic process (A.2) can be computed analytically and are given by

$$\begin{aligned} M_1^U(t) = \mathbb{E}[U(t,X)] &= \tfrac{1}{2} U_0 e^{-v\overline{\sigma}_a t} \frac{e^{v\hat{\sigma}_s t} - e^{-v\hat{\sigma}_s t}}{\hat{\sigma}_s t v}, \\ M_2^U(t) = \mathbb{E}[U^2(t,X)] &= \tfrac{1}{4} U_0^2 e^{-2v\overline{\sigma}_a t} \frac{e^{2v\hat{\sigma}_s t} - e^{-2v\hat{\sigma}_s t}}{\hat{\sigma}_s t v}, \\ \mathbb{V}[U](t) &= M_2^U(t) - (M_1^U(t))^2. \end{aligned} \tag{A.3}$$

Of course, higher order moments, probability of failure, complete characterisation of the probability density function of the stochastic process can be calculated but in figure 1, we focus on the variance $\mathbb{V}[U](t)$ to perform the convergence studies. Note that in practice, we take $v = 1, U_0 = 1, \sigma_t = \overline{\sigma}_s = 0.1, \hat{\sigma}_s = 0.1$. The L^1-norm of the error is computed at time $t = 10$. The curves of figure 1 implying an MC scheme are averaged over 128 computations with different seeds.

Appendix B. The semi-analog and the non-analog MC schemes

In this section, we briefly recall how the semi-analog and the non-analog MC schemes are built and how they are implemented. The schemes are well-known in the literature. Still, we recall their constructions here for the sake of reproducibility of the results but above all because the analysis of sections 3 and 4 begins with the respective *expectation forms* of equation (1) for the different MC schemes. Those forms are presented in the two next sections for the semi-analog MC scheme (see section Appendix B.1) and for the non-analog one (see section Appendix B.2).

Appendix B.1. Construction of the semi-analog MC scheme

The first step in order to rewrite (the deterministic counterpart of) (1) as an expectation consists in identifying a probability measure relative to the time integration in equation (1). By successive

changes of variables and integrations, see [34] for example, (1) can be rewritten (on an infinite domain)

$$\begin{aligned} &u(x,t,v) = \\ &+\int_t^\infty u_0(x-vt,v)v\sigma_t(x-vs,t-s,v)e^{-\int_0^s v\sigma_t(x-v\alpha,t-\alpha,v)\,\mathrm{d}\alpha}\,\mathrm{d}s \\ &+\int_0^t e^{-\int_0^s v\sigma_t(x-v\alpha,t-\alpha,v)\,\mathrm{d}\alpha}\int v\sigma_s(x-vs,t-s,v,v')u(x-vs,t-s,v')\,\mathrm{d}v'\,\mathrm{d}s. \end{aligned} \tag{B.1}$$

It is then possible to factorize by

$$f_\tau(x,t,v,s)\,\mathrm{d}s = \mathbf{1}_{[0,\infty[}(s)v\sigma_t(x-vs,t-s,v)e^{-\int_0^s v\sigma_t(x-v\alpha,t-\alpha,v)\,\mathrm{d}\alpha}\,\mathrm{d}s.$$

The above expression is a probability measure $\forall(x,t,v)\in\mathcal{D}\times[0,T]\times\mathbb{R}^3$: indeed, it is positive and sums up to 1 $\forall(x,t,v)\in\mathcal{D}\times[0,T]\times\mathbb{R}^3$. Using its expression in (B.1) leads to

$$u(x,t,v) = \iint \begin{bmatrix} +\mathbf{1}_{[t,\infty[}(s) & u_0(x-vt,v) & \delta_v(v') \\ +\mathbf{1}_{[0,t]}(s) & u(x-vs,t-s,v') & \dfrac{\sigma_s(x-vs,t-s,v,v')}{\sigma_t(x-vs,t-s,v)} \end{bmatrix} f_\tau(x,t,v,s)\,\mathrm{d}s\,\mathrm{d}v'. \tag{B.2}$$

Without loss of generality, we can write

$$v\sigma_s(x-vs,t-s,v,v') = v\sigma_s(x-vs,t-s,v)P_s(x-vs,t-s,v,v').$$

In the above expression, $\forall(\mathbf{y},\beta)\in\mathcal{D}\times[0,T]$ we have

$$\begin{aligned} \sigma_s(\mathbf{y},\beta,v) &= \int \sigma_s(\mathbf{y},\beta,v,v')\,\mathrm{d}v', \\ P_s(\mathbf{y},\beta,v,v') &= \frac{\sigma_s(\mathbf{y},\beta,v,v')}{\sigma_s(\mathbf{y},\beta,v)}. \end{aligned} \tag{B.3}$$

The quantity $P^s_{\mathbf{V}'}(x,t,s,v,v')\,\mathrm{d}v' = P_s(x-vs,t-s,v,v')\,\mathrm{d}v'$ is positive and is summing up to 1. It is consequently a three-dimensional probability measure $\forall(x,t,v)\in\mathcal{D}\times[0,T]\times\mathbb{R}^3$. The probability measure for the samplings of the velocity $\mathbf{V}'$ is here *averaged over the set of reactions* $r\in\{0,...,R\}$, see [34] for more details. Equation (B.2) can then be rewritten

$$\begin{aligned} &u(x,t,v) = \\ &\iint \begin{bmatrix} +\mathbf{1}_{[t,\infty[}(s) & u_0(x-vt,v) & \\ +\mathbf{1}_{[0,t]}(s) & u(x-vs,t-s,v') & \dfrac{\sigma_s(x-vs,t-s,v)}{\sigma_t(x-vs,t-s,v)}P^s_{\mathbf{V}'}(x,t,s,v,v') \end{bmatrix} f_\tau(x,t,v,s)\,\mathrm{d}s\,\mathrm{d}v'. \end{aligned} \tag{B.4}$$

Introduce the following random variables associated to the previously identified probability measures

$$\begin{cases} \tau & \text{with probability measure} \quad f_\tau(x,t,v)\,\mathrm{d}s, \\ \mathbf{V}' & \text{with probability measure} \quad P^s_{\mathbf{V}'}(x,t,s,v,v')\,\mathrm{d}v'. \end{cases} \tag{B.5}$$

Then (B.4) can be rewritten *in an adjoint recursive way* as an expectation over the above set of random variables (B.5)

$$u(x,t,v) = \mathbb{E}\left[\ \mathbf{1}_{[t,\infty[}(\tau)u_0(x-vt,v) + \mathbf{1}_{[0,t]}(\tau)\frac{\sigma_s(x-v\tau,t-\tau,v)}{\sigma_t(x-v\tau,t-\tau,v)}u(x-v\tau,t-\tau,\mathbf{V}')\ \right]. \tag{B.6}$$

The above expression is the starting point of the analysis of the variance of the semi-analog MC scheme in section 3.2.1.

In order to build the semi-analog MC scheme, it remains to consider a 'particle' solutions $(u_p)_{p\in\{1,\dots,N_{MC}\}}$ of (B.6) having the particular form

$$u_p(x,t,v) = w_p(t)\delta_x(x_p(t))\delta_v(v_p(t)), \tag{B.7}$$

and plug them into (B.6) to identify the operations to perform to make sure each $(u_p)_{p\in\{1,\dots,N_{MC}\}}$ is solution of (B.6). Practically, the above system of equation in term of weight, position and velocity leads to the recursive numerical treatment/algorithm (we here detailed the adjoint formulation) summed up in algorithm 1.

set $u(x,t,v) = 0$
set $u^2(x,t,v) = 0$
for $p \in \{1, ..., N_{MC}\}$ **do**
  set $s_p = t$ *#this will be the remaining life time of particle p*
  set $x_p = x$
  set $\mathbf{v}_p = \mathbf{v}$
  set $w_p(t) = \dfrac{1}{N_{MC}}$
  while $s_p > 0$ **do**
    if $x_p \notin \mathcal{D}$ **then**
      #here a general function for the application of arbitrary boundary conditions
      apply_boundary_conditions$(x_p, s_p, \mathbf{v}_p)$
    end
    Sample τ from the distribution having probability measure $f_\tau(x_p, s_p, s, v_p)\,\mathrm{d}s$.
    if $\tau > s_p$ **then**
      #move the particle p
      $x_p \longleftarrow x_p + \mathbf{v}_p s_p$,
      #set the life time of particle p to zero:
      $s_p \longleftarrow 0$
      #tally the contribution of particle p for the first moment
      $u(x,t,v) += w_p \times u_0(x_p, v_p)$
      #tally the contribution of particle p for the second moment
      $u^2(x,t,v) += w_p \times u_0^2(x_p, v_p)$
    end
    else
      #change the particle weight
      $w_p \longleftarrow \dfrac{\sigma_s(x_p, s_p - \tau, v_p)}{\sigma_t(x_p, s_p - \tau, v_p)} w_p$
      #Sample the velocity $\mathbf{V}'$ *of particle p from* $P^s_{\mathbf{V}'}(x_p, s_p, \tau, v_p, v')\,\mathrm{d}v'$
      $v_p = \mathbf{V}'$
      #move the particle p
      $x_p \longleftarrow x_p + v\tau$,
      #set the life time of particle p to:
      $s_p \longleftarrow s_p - \tau > 0$
    end
  end
end

Algorithm 1: The MC semi-analog scheme described in term of algorithmic operations in order to compute (adjoint) $u(x,t,v)$.

The description of algorithm 1 deduced from the recursive set of equations (B.6) shows that the semi-analog MC scheme is defined by a set of samplings depending on almost every variables x, t, v, v'. The sampling of the velocity $\mathbf{V}'$ is averaged and the weight of the particle is multiplied by the ratio $\frac{\sigma_s}{\sigma_t}$ at the position and at the instant of the shock. The latter ratio corresponds to the probability for the particle of being scattered. The MC particle does not represent the behaviour of a physical particle at x, t, v but rather the behaviour of a population of physical particles at x, t, v. With this treatment, the weight of an MC particle never goes to zero if $\sigma_s \neq 0$. An MC particle is

never explicitly captured hence the denomination 'implicit capture' for this scheme.

The first and second order moments of the solution can be computed during the MC resolution. The instrumentation of the tracking corresponds to the tallying phases (i.e. the $+=$ operations in algorithm 1).

Appendix B.2. Construction of the non-analog MC scheme

In this section, we describe the non-analog scheme, intensively applied in photonic ones. As in the previous sections, we first rewrite the linear Boltzmann equation (1) in an integral form. The non-analog one is obtained from different changes of variables which are detailed in [34].

First, as in the previous section, we rewrite the scattering cross-section

$$v\sigma_s(x-vs,t-s,v,v') = v\sigma_s(x-vs,t-s,v)P_s(x-vs,t-s,v,v').$$

In the above expression, $\forall(\mathbf{y},\beta)\in\mathcal{D}\times[0,T]$ we have

$$\begin{aligned}\sigma_s(\mathbf{y},\beta,v) &= \int \sigma_s(\mathbf{y},\beta,v,v')\,\mathrm{d}v',\\ P_s(\mathbf{y},\beta,v,v') &= \frac{\sigma_s(\mathbf{y},\beta,v,v')}{\sigma_s(\mathbf{y},\beta,v)}.\end{aligned} \tag{B.8}$$

The quantity $P^s_{\mathbf{V}'}(x,t,s,v,v')\,\mathrm{d}v' = P_s(x-vs,t-s,v,v')\,\mathrm{d}v'$ is positive and is summing up to 1. It is consequently a three-dimensional probability measure $\forall(x,t,v)\in\mathcal{D}\times[0,T]\times\mathbb{R}^3$. It is the same as for the semi-analog scheme. The non-analog scheme now needs the introduction of

$$\sigma_a = \sigma_t - \sigma_s.$$

The quantity σ_a is not always equal to the absorption cross-section σ_0 (cross-section of multiplicity $\nu_0 = 0$). It is the case only for a particular set of reactions of the form $r\in\{0,1\}$. Let us decompose σ_t into $\sigma_a+\sigma_s$. This allows making the term $e^{-\int_0^s v\sigma_a(x-v(t-\alpha),\alpha,v)\,\mathrm{d}\alpha}$ appear in factor of u in (B.2). Now using the fact that

$$e^{-\int_0^t v\sigma_s(x-v(t-\alpha),\alpha,v)\,\mathrm{d}\alpha} = e^{-\int_0^t v\sigma_s(x-v\alpha,t-\alpha,v)\,\mathrm{d}\alpha} = \int_t^\infty v\sigma_s(x-vs,t-s,v)e^{-\int_0^s v\sigma_s(x-v\alpha,t-\alpha,v)\,\mathrm{d}\alpha}\,\mathrm{d}s,$$

equation (B.2) rewrites

$$\begin{aligned}u(x,t,v) = &\\ &+\int_t^\infty u_0(x-vt,v)e^{-\int_0^s v\sigma_a(x-v\alpha,t-\alpha,v)\,\mathrm{d}\alpha}v\sigma_s(x-vs,t-s,v)e^{-\int_0^s v\sigma_s(x-v\alpha,t-\alpha,v)\,\mathrm{d}\alpha}\,\mathrm{d}s\\ &+\int_0^t\left[\begin{array}{l} v\sigma_s(x-vs,t-s,v)e^{-\int_0^s v\sigma_s(x-v\alpha,t-\alpha,v)\,\mathrm{d}\alpha}e^{-\int_0^s v\sigma_a(x-v\alpha,t-\alpha,v)\,\mathrm{d}\alpha}\\ \times\iint P_s(x-vs,t-s,v,v')u(x-vs,t-s,v')\,\mathrm{d}v'.\end{array}\right]\mathrm{d}s.\end{aligned} \tag{B.9}$$

It is then possible to factorize by

$$f_\tau(x,t,v,s)\,\mathrm{d}s = \mathbf{1}_{[0,\infty[}(s)v\sigma_s(x-vs,t-s,v)e^{-\int_0^s v\sigma_s(x-v\alpha,t-\alpha,v)\,\mathrm{d}\alpha}\,\mathrm{d}s. \tag{B.10}$$

It is also a probability measure (with respect to σ_s rather than σ_t). We then rewrite the linear Boltzmann equation in another integral form

$$u(x,t,v) = \iint \begin{bmatrix} \mathbf{1}_{[t,\infty[}(s) & u_0(x-vt,v) & e^{-\int_0^s v\sigma_a(x-v\alpha,t-\alpha,v)\,\mathrm{d}\alpha} & \delta_v(v') \\ \mathbf{1}_{[0,t]}(s) & u(x-vs,t-s,v') & e^{-\int_0^s v\sigma_a(x-v\alpha,t-\alpha,v)\,\mathrm{d}\alpha} & P_s(x-vs,t-s,v,v') \end{bmatrix} \times f_\tau(x,t,v,s)\,\mathrm{d}v'\,\mathrm{d}s. \tag{B.11}$$

Integral form (B.11) obtained here is different from the one used for the previous scheme. It mainly differs due to the exponential term multiplying u_0 and u. Let us now introduce the random variables

$$\begin{cases} \tau & \text{with probability measure} \quad f_\tau(x,t,v)\,\mathrm{d}s, \\ \mathbf{V}' & \text{with probability measure} \quad P^s_{\mathbf{V}'}(x,t,s,v,v')\,\mathrm{d}v'. \end{cases} \tag{B.12}$$

Equation (B.11) can then be rewritten *in an adjoint recursive way* as an expectation over the above set of non-analog random variables (B.12)

$$u(x,t,v) = \mathbb{E}\begin{bmatrix} +\mathbf{1}_{[t,\infty[}(\tau) & e^{-\int_0^t v\sigma_a(x-v\alpha,t-\alpha,v)\,\mathrm{d}\alpha} & u_0(x-vt,v) \\ +\mathbf{1}_{[0,t]}(\tau) & e^{-\int_0^\tau v\sigma_a(x-v\alpha,t-\alpha,v)\,\mathrm{d}\alpha} & u(x-v\tau,t-\tau,\mathbf{V}') \end{bmatrix}. \tag{B.13}$$

The above expression is the starting point of the analysis of the variance of the semi-analog MC scheme in section 3.2.2.

In order to build the non-analog MC scheme, it remains to consider a 'particle' solutions $(u_p)_{p\in\{1,\dots,N_{MC}\}}$ of (B.13) having the particular form

$$u_p(x,t,v) = w_p(t)\delta_x(x_p(t))\delta_v(v_p(t)), \tag{B.14}$$

and plug them into (B.13) to identify the operations to perform to make sure each $(u_p)_{p\in\{1,\dots,N_{MC}\}}$ is solution of (B.13).

Practically, the above system of equation in term of weight, position and velocity leads to the recursive numerical treatment/algorithm (we here detailed the adjoint formulation) summed up in algorithm 2.

set $u(x,t,v)=0$
set $u^2(x,t,v)=0$
for $p=1\in\{1,...,N_{MC}\}$ **do**
  set $s_p=t$ *#this will be the life time of particle p*
  set $x_p=x$
  set $\mathbf{v}_p=\mathbf{v}$
  set $w_p(t)=\dfrac{1}{N_{MC}}$
  while $s_p>0$ **do**
    if $x_p\notin\mathcal{D}$ **then**
      #here a general function for the application of arbitrary boundary conditions
      apply_boundary_conditions$(x_p,s_p,\mathbf{v}_p)$
    end
    Sample τ from the distribution having probability measure $f_\tau(x_p,s_p,s,v_p)\,\mathrm{d}s$.
    if $\tau>s_p$ **then**
      #change its weight
      $w_p\longleftarrow e^{-\int_0^{s_p}v_p\sigma_a(x_p-v_p\alpha,s_p-\alpha,v_p)\,\mathrm{d}\alpha}w_p$
      #move the particle p
      $x_p\longleftarrow x_p+\mathbf{v}_p s_p,$
      #set the life time of particle p to zero:
      $s_p\longleftarrow 0$
      #tally the contribution of particle p
      $u(x,t,v)+=w_p\times u_0(x_p,v_p)$
      #tally the contribution of particle p for the second moment
      $u^2(x,t,v)+=w_p\times u_0^2(x_p,v_p)$
    end
    else
      #change the particle weight
      $w_p\longleftarrow e^{-\int_0^{\tau}v_p\sigma_a(x_p-v_p\alpha,s_p-\alpha,v_p)\,\mathrm{d}\alpha}w_p$
      #Sample the velocity $\mathbf{V}'$ *of particle p from* $P^s_{\mathbf{V}'}(x_p,s_p,\tau,v_p,v')\,\mathrm{d}v'$
      $v_p=V'$
      #move the particle p
      $x_p\longleftarrow x_p+v_p\tau,$
      #set the life time of particle p to:
      $s_p\longleftarrow s_p-\tau>0$
    end
  end
end

Algorithm 2: The MC non-analog scheme described in term of algorithmic operations in order to compute (adjoint) $u(x,t,v)$.

Algorithm 2 mainly differs from the previous one (algorithm 1) by the fact that

– the interaction time is sampled from σ_s rather than from σ_t,

– the weight of the particle is modified along its flight path.

The sampling of the velocity $\mathbf{V}'$ is averaged over the set of reactions at the position and at the instant of the interaction. Once again, the MC particle does not represent the behaviour of a

physical particle at x, t, v but rather the behaviour of a population of physical particles at x, t, v averaged in a homogeneous media. Indeed, the weight modification along the flight path of a particle corresponds to the solution of a punctual/homogeneous problem given by

$$\partial_s U_{x,t,v}(s) = -v\sigma_a(x - vs, t - s, v)U_{x,t,v}(s). \tag{B.15}$$

It is equivalent to having

$$\frac{U_{x,t,v}(t)}{U_{x,t,v}(0)} = e^{-\int_0^t v\sigma_a(x-v\alpha,t-\alpha,v)\,\mathrm{d}\alpha}, \tag{B.16}$$

and exactly corresponds to the weight modification along the flight path of each MC particles. The asymptotic property of the scheme will be emphasized in section 3.2.2.

The first and second order moments of the solution can be computed during the MC resolution. The instrumentation of the tracking corresponds to the tallying phases (i.e. the $+=$ operations in algorithm 2).

Appendix C. The MC-gPC schemes

In this section, we build and express the gPC based reduced model of (1) as an expectaction over a set of random variables. This set of random variables additionally contains the uncertain variable X. This section is fully detailed in [2] and [1] but we recall the construction of the reduced model and of the MC scheme in this paper for the sake of reproducibility of the results. Still, care is taken to suggest a new way to present MC-gPC in a general manner: the algorithms of this section explain how we can implement both the non-analog and the semi-analog MC schemes in the same MC-gPC code.

The gPC reduced model of the uncertain transport equation (1) of size $P+1$ is given by (we drop the dependencies for convenience)

$$\left\{\begin{array}{ll} \partial_t u_0 + v\cdot\nabla_x u_0 & = -v\displaystyle\int\left(\sigma_t\sum_{k\le P}u_k\phi_k\right)\phi_0\,\mathrm{d}\mathcal{P}_X + v\iint\left(\left(\sigma_s\sum_{k\le P}u_k\phi_k\right)\phi_0\,\mathrm{d}\mathcal{P}_X\right)\,\mathrm{d}v', \\ \dots & \dots \\ \partial_t u_P + v\cdot\nabla_x u_P & = -v\displaystyle\int\left(\sigma_t\sum_{k\le P}u_k\phi_k\right)\phi_P\,\mathrm{d}\mathcal{P}_X + v\iint\left(\left(\sigma_s\sum_{k\le P}u_k\phi_k\right)\phi_P\,\mathrm{d}\mathcal{P}_X\right)\,\mathrm{d}v'. \end{array}\right. \tag{C.1}$$

It is obtained from a Galerkin projection of (1) onto the gPC basis $(\phi_k)_{k\in\{0,\dots P\}}$, see [2].

Going through the same steps as in Appendix B.1, the expectaction form of system (C.1) writes $\forall k \in \{0, ..., P\}$

$$u_k(x,t,v) = \mathbb{E}\left[\begin{array}{ll} + & \mathbf{1}_{[t,\infty[}(\tau_X)u_0(x-vt,v,X)\phi_k(X) \\ + & \mathbf{1}_{[0,t]}(\tau_X)u(x-v\tau_X,t-\tau_X,\mathcal{V}_X,X)\dfrac{\sigma_s(x-v\tau_X,t-\tau_X,v,X)}{\sigma_t(x-v\tau_X,t-\tau_X,v,X)}\phi_k(X) \end{array}\right]. \tag{C.2}$$

Note that the complete description of the steps leading to (C.2) is available in [1].

for $k \in \{0, ..., P\}$ **do**
  set $u_k(x,t,v) = 0$
  set $u_k^2(x,t,v) = 0$
end
for $p = 1 \in \{1, ..., N_{MC}\}$ **do**
  set $s_p = t$ *#this will be the life time of particle p*
  set $x_p = x$
  set $v_p = v$
  set $\mathbf{X}_p \sim \mathbf{X}$
  set $w_p(t) = \dfrac{1}{N_{MC}}$
  while $s_p > 0$ **do**
    if $x_p \notin \mathcal{D}(X_p)$ **then**
      #here a general function for the application of arbitrary boundary conditions
      apply_boundary_conditions$(x_p, s_p, v_p, \mathbf{X}_p)$
    end
    sample $\tau =$ sample_interaction_time(x_p, v_p, X_p)
    $K =$ compute_weight_modif$(x_p,\ v_p,\ \tau,\ \tau_{census},\ \tau_{exit},\ \tau_{inter}, X_p)$
    $w_p \longleftarrow K \times w_p$
    if $\tau > s_p$ **then**
      #move the particle p
      $x_p \longleftarrow x_p + v_p s_p,$
      #set the life time of particle p to zero:
      $s_p \longleftarrow 0$
      #tally the contribution of particle p for the first and second moments
      for $k \in \{0, ..., P\}$ **do**
        $u_k(x,t,v) += w_p \times u_0(x_p, v_p, X_p)\phi_k(X_p)$
        $u_k^2(x,t,v) += w_p \times [u_0(x_p, v_p, X_p)\phi_k(X_p)]^2$
      end
    end
    else
      #Sample the velocity $\mathbf{V}'$ *of particle p from* $P^s_{\mathbf{V}'}(x_p, s_p, \tau, v_p, v', X_p)\,\mathrm{d}v'$
      $v_p = V'$
      #move the particle p
      $x_p \longleftarrow x_p + v_p \tau,$
      #set the life time of particle p to:
      $s_p \longleftarrow s_p - \tau > 0$
    end
  end
end

Algorithm 3: The semi-analog and non-analog MC-gPC schemes described in term of algorithmic operations in order to compute (adjoint) $u(x,t,v,X)$.

The tracking phase allowing to solve (C.2) is described in algorithm 3. It describes the 'tracking' of an uncertain population of particles within the simulation domain $\mathcal{D}$ In order to present both implementations (of the semi-analog and non-analog MC schemes) in the same general framework/-code, we encapsulated some key parts of the resolution in several functions: sample_interaction_time,

compute_weight_modif, sample_velocity[16]. The three latter key functions are described in algorithms 4–5–6 but for the moment let us focus on the common canvas (i.e. algorithm 3).

sample_interaction_time(real x, real v, real X)
set τ = REAL_MAX
U =sample_uniform_law()
if $MC\_scheme == semi - analog$ **then**
  $\tau = -\dfrac{\ln(U)}{v\sigma_t(x,v,X)}$
end
if $MC\_scheme == non - analog$ **then**
  $\tau = -\dfrac{\ln(U)}{v\sigma_s(x,v,X)}$
end
return τ

Algorithm 4: The sampling of the interaction time function depending on the choice of the MC scheme

sample_velocity(real x, real v, real X)
$\mathbf{V}'$ =sample_from_$P_s(x,v,X)$
return $\mathbf{V}'$

Algorithm 5: Sampling of the velocity

In algorithm 3, we can see that each presented scheme relies on comparing three times, τ_{inter} the interaction time, τ_{exit} the time at which an MC particle p would get out of the cell i_p, τ_{census} the time before ending the time step. For each scheme, the particle moves along $v_p\tau$ where τ is the minimum of the three above times. Its weight is modified or not (in compute_weight_modif) depending on the scheme. Furthermore, depending on the minimum of $\tau_{census}, \tau_{exit}, \tau_{inter}$, the particle sees its life time updated and finishes its treatment (*census*) or crosses the interface between two cells (*exit*) or encounters an interaction (*inter*). In the latter case, its velocity change. All the samplings potentially depends on the uncertain field X_p carried out by the uncertain MC particle p. The first and second order moments of the gPC coefficients are computed during the MC resolution. The instrumentation of the tracking corresponds to the tallying phases (i.e. the $+=$ operations in algorithm 3).

Let us now focus on the encapsulated functions. First, note that they all only depend on particle fields $(x_p, v_p, i_p, X_p, ...)$. The first one, to sample the interaction time, only needs the particle energy v_p and the uncertain one X_p and is detailed in algorithm 4. Depending on the chosen scheme, the interaction time is sampled from the total cross-section σ_t (semi-analog) or from the scattering one σ_s in the current cell i_p. Both are obtained inversing the cdf of an exponential law.

The second encapsulated function corresponds to the modification of the weight of the particle, detailed in algorithm 6. For this function, the event the particle encounters explicitly appears in the treatment. The non-analog scheme is the only one having a treatment independent of the event. The weight of a particle remains unchanged for the semi-analog schemes for the *census* and *cell exit* events. It changes in the case of an interaction: for the semi-analog scheme, the weight is multiplied by the probability of being scattered $\frac{\sigma_s}{\sigma_t}$.

[16]We do not detail the functions compute_cell_exit_time and find_neighbooring_cell as they depend more on the type of grid (cartesian, structured, unstructured) than on the MC resolution scheme.

compute_weight_modif(real v**, real** $\tau_{\min}$**, real** τ_{census}**, real** τ_{exit}**, real** τ_{inter}**, integer** i**, real** X**)**
set $K = 1$
if $MC\_scheme == semi - analog$ **then**
  if $\tau_{\min} == \tau_{exit}$ *or* $\tau_{\min} == \tau_{census}$ **then**
    $K = 1$
  end
  if $\tau_{\min} == \tau_{inter}$ **then**
    $K = \dfrac{\sigma_s^i(v, X)}{\sigma_t^i(v, X)}$
  end
end
if $MC\_scheme == non - analog$ **then**
  $K = e^{-v(\sigma_t^i(v,X) - \sigma_s^i(v,X))\tau_{\min}}$
end
return K, r

Algorithm 6: The weight modification depending on the MC scheme

At the interaction time, each scheme needs the sampling of the outer velocity $\mathbf{V}'$, summed up in algorithm 5. The semi-analog and the non-analog schemes share the same procedure, using P_s, averaged over the set of reactions $r \in \{0, ..., N_R\}$.

In algorithm 3, time steps are explicitly detailed but for the linear Boltzmann equation, time steps may coincide with the times of interest (MC methods are inconditionally stable for the linear Boltzmann equation). In other words, if one is only interested in time T, it is possible choosing $\Delta t = T$. This is not the case in [6, 7] in which the coupling with additional equations induces restrictions on the time step. Note that the above algorithm description still applies for the MC resolution of the linear Boltzmann equation coupled to other equations but may need additional instrumentations (track length estimator for example).

To finish, we add that the tracking phase as described in algorithm 3 is commonly denoted 'history-based'. It refers to the fact that during one time step, an MC particle is followed from $s_p = t - \Delta t$, i.e. the beginning of the new time step, until $s_p = t$, i.e. the end of the current time step (if, of course, the MC particle is not killed during its history[17]). Another possibility would be to apply the events one by one to the whole population of particles until they all reach census or die, this is what is commonly called an 'event-based' tracking phase. These considerations are practical ones and do not explicitly depend on the applied MC scheme. Nevertheless, the discussion on the choice of a 'history-based' tracking or an 'event-based' one is far from being irrelevant as the target computation device (one may have access to a station, a computation cluster, a supercomputer, with homogeneous nodes or hybrid ones...) may be sensitive to the operations induced by the two possibilities. Hybrid architectures (classical nodes, GP-GPU units, vectorization) becoming more and more common, hybrid strategies mixing history-and-event-based tracking phases may become more and more relevant. The discussion is beyond the scope of this document but is very interesting and we refer to [31] for some examples of fine-coarse grain parallel strategies for the linear Boltzmann equation.

[17] depending on the chosen MC scheme.